A Comparative Study of Infrared Thermography (IRT) And Radio Frequency Identification (RFID) as Methods to Measure Moisture Levels in Adobe Walls

Chongke Wu

A THESIS

in

Historic Preservation

Presented to the Faculties of the University of Pennsylvania in

Partial Fulfillment of the Requirements of the Degree of

MASTER OF SCIENCE IN HISTORIC PRESERVATION

2020

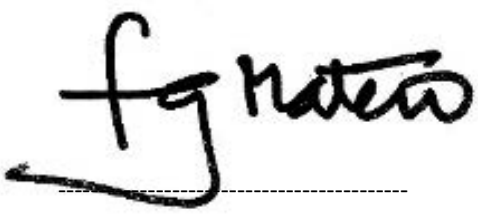

Advisor/Program Chair

Frank Matero

Professor of Architecture

Acknowledgements

In the process of completing this thesis, I have received the help of many people and organizations. I could not have completed this project without my family, advisor and close friends. Many thanks to the following people for their guidance and support.

To my advisor, Frank Matero, for guiding me through this thesis process. Thank you for dedicating your time to help develop this test procedure. Thank you for all the helpful advice.

To those who helped with the design of the test and preparation of testing equipment. Thank you to John Hinchman for helping me design the sand columns and for generously lending me the infrared camera. Thank you to Evan Oskierko – Jeznacki for teaching me a lot about IRT and RFID, and for helping me to refine my thesis. Thank you to Courtney Magill, lab manager for the Architectural Conservation Laboratory, for providing me guidance and test equipment.

To Convergence Systems Limited for providing the C108 RFID reader for free. To Smartrac® for providing a lot of RFID tags for my test.

Lastly, thank you to my friends and family for your continuous support and love. Thank you to my parents for allowing me this great opportunity. To my classmate Zhen Ni, thanks for helping and accompanying me.

Table of Contents

List of Figures

List of Tables

Chapter 1 : Introduction

This thesis investigation began with an interest in understanding the moisture issues faced at Fort Union Historic Monument and Pecos National Historic Park in the American Southwest, two projects I was involved with during my summer internship at the Center for Architectural Conservation (CAC) at the Weitzman School of Design, University of Pennsylvania. For most adobe structures, and especially those located in the American Southwest, increased exposure to moisture is becoming a serious threat due to climate change. The goal of this thesis is to provide useful data along with a useful diagnostic methodology to inform stewards of traditional adobe structures of a low cost and minimally invasive method for measuring the moisture content in adobe walls. The most widely used methods of accurately measuring the moisture content of porous materials are based on gravimetric analysis involving the removal of samples of historic fabric and comparing the 'as found' weight to the optimal dry weight in the lab. The question posed for this thesis is: can an infrared camera in conjunction with RFID tags be used to quantitatively determine and monitor in situ moisture content of an adobe wall?

This research begins with a brief review of the manufacturing techniques and properties of adobe in Chapter 2. This chapter addresses the composition, production process, and critical physical and mechanical properties of adobe systems. Chapter 3 : Moisture Related Deterioration of Adobe Building discusses moisture-related deterioration mechanisms and the severe damage that will result without appropriate

treatments. It's worth noting that most moisture-related decay processes take place simultaneously albeit at different scales and rates. The remedying of only one of these will not necessarily arrest deterioration if others are left untreated.

To mitigate moisture damage in buildings, professionals use a range of nondestructive, moderately destructive, and destructive tools. Chapter 4 : A Survey of Existing Tools Used in the Field to Measure Moisture Content Levels in Historic Structures provides a literature review for the tools and procedures executed by professionals on historic structures. In addition to the most commonly used methods such as electrical techniques, infrared thermography (IRT) and radio frequency identification (RFID) techniques are becoming increasingly popular for their non/low-destructive nature and ability to recognize moisture anomalies in historic building materials over a large area. Therefore, Chapter 5 introduces in greater detail infrared thermography (IRT) and radio frequency identification (RFID) for recognizing moisture anomalies in building diagnostics.

Currently, both IRT and RFID are indirect methods of measuring moisture and display ranges and limitations that need to be better understood for adobe. Verification of true moisture levels in a wall requires localized in situ readings with a moisture meter and gravimetric analysis of removed samples that directly measures water content using laboratory procedures. The testing methodology designed for this thesis aims to compare IRT and RFID methods on loose porous bodies (sand columns) as a simulacrum for adobe brick and to compare those results to standard direct methods such as

gravimetric analysis to identify tolerances and limitations for each method on the material. From the results and conclusions of this experiment, a set of recommendations has been generated for refining the laboratory methodology and for future application of this method in the field.

Chapter 2 : A Brief Review of Adobe and its Properties

Mudbrick or adobe is one of the oldest and most widespread building materials in the world, dating as far back as the 8th century B.C. It was used in the southern Mediterranean, where it was first introduced by the Moors during their occupation of southern Spain and it was the Spaniards who exploited its use in the Americas upon their arrival[1]. In the United States, many examples of historic adobe architecture can be found, especially in the southwestern states. Santa Fe, New Mexico, for example, has many adobe structures, including the Palace of the Governors, which dates to the early 17th century.

Traditional adobe is composed of sand, sometimes gravel, clay, water, and often straw or grass mixed together, formed in wooden molds, and dried by the sun.. Although the straw and grass do not help to strengthen the bricks or to give them added long-term durability, they do help the bricks shrink more uniformly while they dry[2]. Today some commercially available adobe-like bricks are fired. These are similar in size to unbaked bricks, but have a different texture, color, and strength. Similarly, some

[1] Marchand, Trevor (2009). The Masons of Djenne. Bloomington: University of Indiana Press
[2] U.S. Department of the Interior National Park Service, 1978, “Preservation of Historic Adobe Buildings”, https://www.nps.gov/tps/how-to-preserve/briefs/5-adobe-buildings.htm

adobe bricks have been stabilized, containing cement, asphalt, and/or bituminous materials, but these also differ from traditional adobe in their appearance and strength[3].

Compared to fired brick, mud brick displays low compressive strength and the inability to resist tensile stresses like most masonry materials. In the United States, most building codes[4] call for a minimum compressive strength of 300 lb/in^2 (2.07 newton/mm2) for adobe block.

Table 2.1： Physical requirements of adobe brick

Minimum compressive strength (newton/mm2)	Water absorption (%)	Moisture content (%)	Minimum modulus of rupture
2.113 (Average) 1.760 (Minimum)	2.5	4.0	0.352 (Average) 0.246 (Minimum)

Source: Table 24-B: Uniform Building Code, 1994

In addition to being an inexpensive material with a small resource cost, assuming the raw materials are local, adobe can serve as an excellent heat reservoir due to the thermal properties inherent in the material and its massive walls. In climates typified by hot days and cool nights, the high thermal mass of adobe mediates the high and low temperatures of the day, moderating the temperature of the living space. The massive

[3] U.S. Department of the Interior National Park Service, 1978, “Preservation of Historic Adobe Buildings”, https://www.nps.gov/tps/how-to-preserve/briefs/5-adobe-buildings.htm
[4] Construction Industries Division of the Regulation and Licensing, “2003 New Mexico Earthen Building Materials Code, Title 14, Chapter 7, Part 4”

walls require a large and relatively long input of heat from solar radiation and from the surrounding air convection before they warm through to the interior. After the sun sets and the temperature drops, the warm wall will continue to transfer heat to the interior for several hours due to the time-lag effect. Thus, a well-planned adobe wall of the appropriate thickness is very effective at controlling inside temperature through the wide daily fluctuations typical of desert climates, a factor which has contributed to its longevity as a building material[5].

Due to their air drying and hardening, mud bricks do not permanently harden, thus remaining vulnerable to moisture. Besides water, plant growth, insects and animal activity, and wind can also compromise adobe bricks/walls rendering them prone to failure[6]. It should be cautioned that adobe deterioration is often the end-product of more than one single agent. The remedying of only one of these will not necessarily arrest deterioration if others are left untreated.

Today, although adobe is no longer a prevalent building material, a great many earthen structures remain a significant part of the international building stock. The extensive use of the material over the centuries has led to strong local traditions of building with earth today.

[5] Wikipedia, "Adobe", https://en.wikipedia.org/wiki/Adobe

[6] Illampas, R; Ioannou, I; Charmpis, D, 2013, "Overview of the Pathology, Repair and Strengthening of Adobe Structures", International Journal of Architectural Heritage. Volume 7, Issue 2, pp. 165-188.

Chapter 3 : Moisture-Related Deterioration of Adobe Building

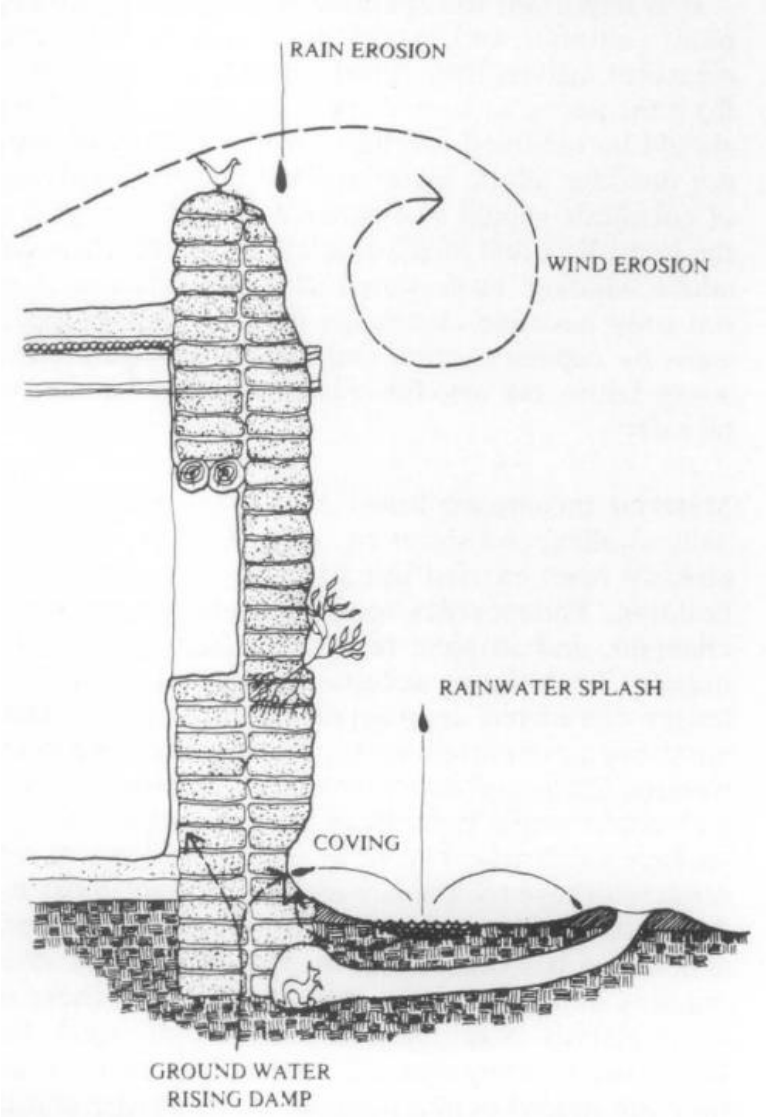

Figure 3.1: adobe deterioration, image from U.S. Department of the Interior National Park Service

Generally, adobe buildings deteriorate mainly because of excessive moisture in the form of rainwater, melting snow, or ground water. Moisture can damage an adobe building from many indirect mechanisms such as freeze thaw and salt crystallization and the deterioration of adobe cannot be attributed to one deterioration mechanism. Most decay processes take place simultaneously and at different scales however moisture is often involved.

Moisture-Driven Disintegration of Adobe Bricks

Disintegration of adobe bricks occurs when the soil constituting the adobes loses its cohesion. This is, in most cases, related to the action of excessive water on the material. Moisture enters adobe structures by several different mechanisms, the most common of which are infiltration and capillary absorption of ground water, wind-driven rainfall, condensation (dew) and everyday building use[7].

Although research[8] has shown that earth-based building materials generally tend to absorb less water by capillarity than conventional masonry materials (e.g., fired clay bricks), the effects of moisture on adobe construction are far more devastating. Moisture primarily affects the clay component which is a key ingredient in making adobes[9]. Clay is cohesive and acts as a binder for all coarser particles within the material's matrix, just as cement does in concrete. In addition, increased humidity causes the natural fibers within the adobe bricks to rot. According to the literature[10], these fibers offer better coherence between the soil layers, and prevent the regions near the surface of the material to fall off when large deformations are induced.

[7] Walker, P. 2002. Australian earth building handbook: HB195–2002, Sydney, Australia: Standards Australia.
[8] Hall, M. and Djerbib, Y. 2004. Moisture ingress in rammed earth: Part 1–The effect of the soil particle–size distribution on the rate of capillary suction. Construction and Building Materials, 18(4): 269–280.
[9] Salles, F., Douillard, J. M., Denoyel, R., Bildstein, O., Jullien, M., Beurroies, I. and Van Damme, H. 2009. Hydration sequence of swelling clays: Evolutions of specific surface area and hydration energy. Journal of Colloid and Interface Science, 333(10): 510–522.
[10] Binici, H., Aksogan, O. and Shah, T. 2005. Investigation of fibre reinforced mud brick as a building material. Construction and Building Materials, 19(4): 313–318.

Therefore, their loss is detrimental to the material's mechanical properties and durability as well.

An additional mechanism by which trapped moisture may cause the disintegration of adobe bricks is cyclic freezing and thawing of water within the pores, within microcracks or just below the surface of earthen materials. Freeze/thaw cycles lead to the development of increased pore pressures that gradually force the soil particles to lose cohesion and cause the material to detach from the structure[11]. The damage induced in an adobe structure due to freezing and thawing depends mainly on the number of cycles and the moisture content of the mud bricks[12].

Many researchers also refer to the role of salt crystallization in the disintegration of adobe bricks. It is reasonable to argue that the degradation of the material's matrix is primarily a product of the action of moisture on the clay particles, rather than the result of the disruptive internal pressure of salt crystallization. However, an examination of adobe samples from various earthen structures has revealed that deteriorated adobe contains considerable amounts of soluble salts within its mass[13]. This finding may be considered as an indication that salt crystallization occurs concurrently with other degradation mechanisms, thus speeding up the rate of decay.

[11] Warren, J. 1998. Conservation of earth structures, Oxford, UK: Butterworth–Heinemann.
[12] Qu, J. J., Cheng, G. D., Zhang, K. C., Wang, J. C., Zu, R. P. and Fang, H. Y. 2007. An experimental study of the mechanisms of freeze/thaw and wind erosion of ancient adobe buildings in Northwest China. Bulletin of Engineering Geology and the Environment, 66(2): 153–169.
[13] Brown, W. P., Robbins, R. C. and Clifton, R. J. 1979. Adobe II: Factors affecting the durability of adobe structures. Studies in Conservation, 24(1): 23–29.

In addition, increased moisture on the surface of earthen materials generates the growth of algae, fungi, mosses, lichens, bacteria, or plants[14]. These organisms affect the material superficially and attack adobe both chemically and physically.

The disintegration of adobe bricks, especially at the base of walls reduces the surface area of the material that can accommodate loading. In extreme cases, this reduction may lead to severe structural problems, since the bearing capacity of masonry walls may potentially be decreased to the point of collapse[15].

Deterioration at the Base of Adobe Walls

Erosion and spalling at the base of walls is a very common form of damage observed in adobe structures. This damage is usually caused by the uptake of ground water by capillary action due to the absence of damp-proof membranes and courses at the foundation level[16]. Basal erosion can also be the result of the splashing of falling rainwater against the wall.

When moisture gets trapped into the base of an adobe wall, it fills the pores of the adobe and mortar, the latter usually also of clay and sand. Depending on the temperature and relative humidity conditions, moisture can evaporate, suffer freeze-thaw cycles, condense or deposit soluble salts within the adobe. Gradually, these mechanisms generate internal cracking and cause the material to lose cohesion and

[14] Warren, J. 1998. Conservation of earth structures, Oxford, UK: Butterworth–Heinemann.
[15] Hammond, A. A. 1973. Prolonging the life of earth buildings in the tropics. Building Research & Information, 1(3): 154–163.
[16] Pearson, G. T. 1994. Conservation of clay and chalk buildings, Shaftesbury, , UK: Donhead Publishing.

disintegrate from the rest of the body; this in turn results in characteristic undercutting within the wet zone. The outcome of the deterioration processes is the formation of continuous deep horizontal fissures at the boundary between the ground or base and the adobe wall. The main problem arising from deterioration at the base of the wall is the loss of support under loading, which introduces load-bearing eccentricities into the structure and may eventually lead to overturning[17].

Figure 3.2: base erosion. image from National Park Service

[17] Aytun, A. 1981. "Earthen buildings in seismic areas of Turkey". In Proceedings of the International Workshop on Earthen Buildings in Seismic Areas, Vol. II, 345–371. Albuquerque, NM: University of New Mexico Press.

Deterioration at the Top of Adobe Walls

When the upper part of an adobe structure is not adequately protected, water penetrates pre-existing micro-cracks formed immediately after drying and worsening over time from the material's expansion and contraction during repeated wetting and drying cycles. As in the case of basal erosion, excessive water will dissociate the clay binder from saturated areas causing mass disintegration, erosion and crack widening. Larger vertical structural cracking induced by seismic action, ground settlement or overloading, and flawed construction (e.g., unbonded wythes) offers a channel for liquid water entry. When water penetrates cracks the deterioration mechanisms described above occur. Deterioration at the top of adobe structures produces a saw-toothed effect laterally observed as serrations[18]. When no measures for the protection and repair of the affected areas are taken, the serrations gradually become wider and progress downwards. Ultimately, large vertical fissures and cracks are formed, and the wall appears as a series of pinnacles standing between eroded zones. As a result, the area of the masonry that can sustain loading is reduced and vertical planes of weakness develop. The latter negatively affects the resistance of the wall to out-of-plane loading and influences the seismic behavior of the structure as well. Deterioration at the top of adobe walls may also induce decay to surface coatings and may lead to the deformation of roof beams and window lintels. The removal of soil particles from the upper part of earthen structures is, in some cases, accentuated by wind action, as surfaces which have

[18] Warren, J. 1998. Conservation of earth structures, Oxford, UK: Butterworth–Heinemann.

lost coherence because of moisture become friable and can be easily disturbed by air moving at high velocities[19].

Successful stabilization, restoration, and the ultimate survival of an adobe building therefore depends upon how effectively a structure sheds water. The importance in keeping an adobe building free from excessive moisture cannot be overstated.

Figure 3.3: deterioration at the top of adobe walls. Image available online

[19] Qu, J. J., Cheng, G. D., Zhang, K. C., Wang, J. C., Zu, R. P. and Fang, H. Y. 2007. An experimental study of the mechanisms of freeze/thaw and wind erosion of ancient adobe buildings in Northwest China. Bulletin of Engineering Geology and the Environment, 66(2): 153–169.

Chapter 4 : A Survey of Existing Tools Used in the Field to Measure Moisture Content Levels in Historic Adobe Structures

Moisture problems within adobe buildings can cause structurally devastating effects. Consequently, the measurement of moisture has been of interest to building professionals for many years. The absorption and transport of water in adobe, perhaps also combined with the effects of air movement through structures, are complex processes. Capillary rise, evaporation, the infiltration of driving rain, as well as surface and interstitial condensation, are examples of the diversity of phenomena involved. Further complications may arise during periods of cold, when freezing and expansion of water can lead to material failure. During dry spells, the evaporation of water may result in efflorescence[20] due to the concentration of salts forming at or near the exterior surfaces. Current climate change predictions[21] indicate that buildings must now be designed to deal with an external environment which is more hostile in terms of moisture loading, with higher winter humidity, more winter driving rain, flooding and increased wind speeds.[22] There is, therefore, a need for suitable moisture measurement techniques to aid the building profession in the diagnosis of building problems and preservationists in acquiring further understanding of moisture transport with a view to improving the future preservation or restoration. This chapter reviews current moisture

[20] Glaser H. Graphical method for investigation of diffusional processes. Kaltetechnik 1959; 11(10): 345–349

[21] UK Climate Impacts Programme. Climate change scenarios for the United Kingdom: The UKCIP02 Briefing Report. Tyndall Centre for Climate Change Research, Norwich, 2002.

[22] Graves HM, Phillipson MC. Potential implications of climate change in the built environment. Foundation for the Built Environment, London, 2000.

measurement practices and some more sophisticated techniques available, and then compares their advantages and limitations when used for in-situ moisture content measurement.

The availability of affordable, user-friendly and portable equipment determines the range of techniques used by most professionals. For specialist applications professionals may have more sophisticated techniques at their disposal. The site or building manager is usually interested in measurement techniques that allow repeatable measurements of the relative moisture content over time. Some of the commercially available devices can produce measurements of absolute moisture content when applied to materials for which they have been previously calibrated. The manufacturer's declared accuracy of measurements applies only to the materials for which the device is calibrated; other materials cannot be measured to the same standards and need to be interpreted as only relative moisture content measurements. The following techniques are the more common approaches currently used in the historic preservation field; the relative advantages and limitations associated with each of these techniques are given in Table 1.

4.1 Sampling Techniques

A simple method for measuring the moisture content of adobe is to drill a hole in the material to be sampled, collect the drilled debris and measure its moisture content gravimetrically by weighing before and after oven drying. Careful application of the drilling technique allows the material to be collected from progressive depths within the

sample, enabling the moisture profile through the material to be measured. To minimize the drying of the sample by heat from drilling, low speed or hand drills can be used.[23]

Moisture content can rapidly be assessed from drillings if a carbide meter is used. This requires the drilled material to be exposed to calcium carbide in a sealed container; the resulting reaction with the moisture in the sample produces a volume of acetylene gas in proportion to the moisture content; this is measured by the rise in pressure in the container[24]. The carbide meter is an alternative solution to the moisture meter for testing and diagnosing damp problems. While both are destructive, carbide meters do give a direct, in situ, and quantitative measurement of moisture in a substance. The destructive nature of both methods limits the number of times that the moisture content can be measured in a location, which makes the technique unsuitable for monitoring and assessing long-term changes in moisture content for historic structures. Furthermore, the carbide meter is mainly used as an onsite testing tool for walls with levels of 5% moisture content or less. which may be a problem for measuring walls with higher moisture content. [25].

[23] S. G. Reynolds, 1970, "The Gravimetric method of Soil Moisture Determination" Journal of Hydrology 11 (1970) P258-273
[24] Moisture Meter Guide, "The Carbide Moisture Meter" http://www.moisturemeterguide.com/page211.html#.XnpXdKhKiUk
[25] Moisture Meter Guide, "The Carbide Moisture Meter" http://www.moisturemeterguide.com/page211.html#.XnpXdKhKiUk

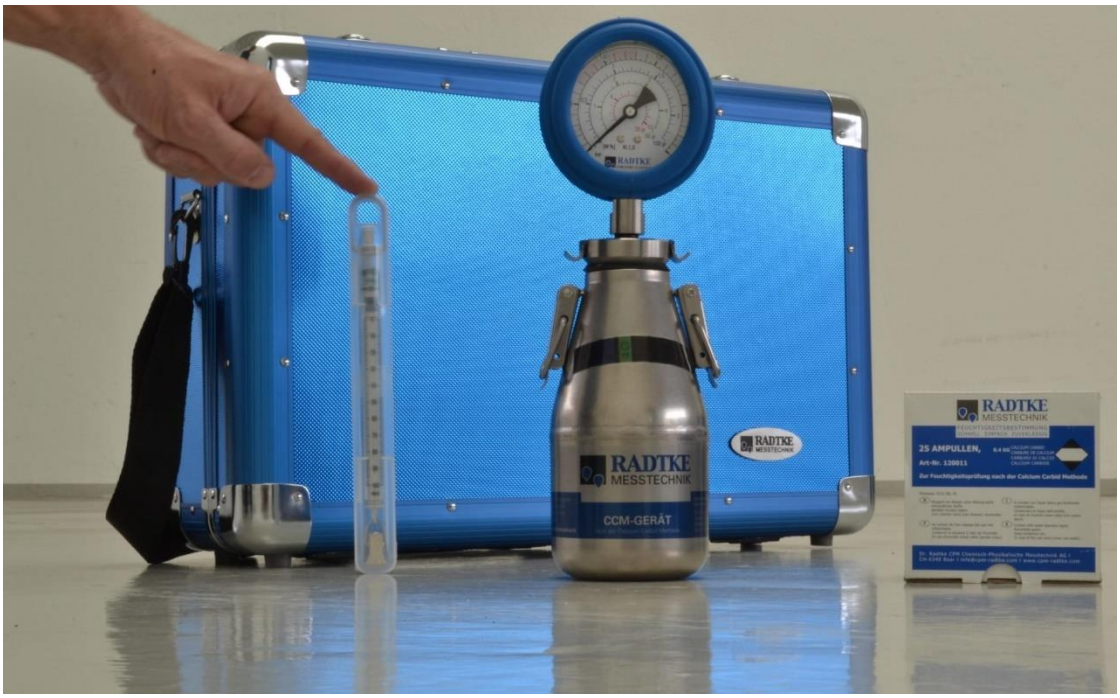

Figure 4.1: Carbide Moisture Meter. image from radtke messtechnik website.

4.2 Electrical Techniques

The relationship between the electrical properties of porous materials and their moisture content is well established[26] Measurements of resistance, impedance, capacitance, and the dielectric constant of porous materials are all influenced by a material's moisture content and all have been used as the basis of assessing moisture content.[27] Commercially available devices use at least one, and sometimes a combination of these properties. While this instrumentation hasbeen developed over the years for a wide range of industrial applications, the transfer of this technology to

[26] Knowler AE. On the measurement of the electrical resistance of porous materials. Proc Phys Soc 1927; 40: 37–40.
[27] Andrae G. The measurement of moisture in concrete. Materialprufung 1973; 15(3): 95–97.

the investigation of building materials still requires carefully designed instrumentation, especially for adobe which is complex and inconsistent material.

Figure 4.2 ： pin-type moisture meter and pinless moisture meter. Image from home depot website.

Electrical properties of materials can be very sensitive to the presence of water; however, good sensor design is important. There are several limiting factors which should be considered before electrical techniques are used. Commercial devices are often calibrated to give an absolute moisture content reading for a generic material, such as timber; readings with other materials give comparative measurements, but

without further calibration they cannot give an accurate absolute measurement of the moisture content. Good electrical contact between the device and the material being measured is essential; for certain materials this can be problematic and give inconsistent measurements. The accuracy and quality of results from electrical techniques are also affected by local temperature variations, the presence of dissolved salts in the pore solution and the presence of metallic components close to the measurement point. Variations and uncertainty in the materials used within the construction also limit the accuracy of these techniques. Commercial microwave moisture meters are available which measure the dielectric constant of the medium in contact with the instrument and can assess the moisture content to a depth of 50 mm (2 inches) into a material.[28] Use of these devices is generally limited to concrete. An advantage is that calibration for different densities of materials is not necessary. However, the presence of metallic components and certain ceramics within the measurement volume can give misleading results.

With appropriate attention to the condition of the material, electrical techniques can offer a quick, non-destructive method of identifying the extent of surface moisture by giving comparative measurements. Therefore, they allow a building professional to assess the extent of a dampness problem quickly with comparative readings across a

[28]Dill MJ. A review of testing for moisture in building elements. Construction Industry Research and Information Association, London, 2000.

surface.[29] They do not enable the determination of the moisture content deep within the wall and only give absolute moisture content for materials which have been pre-calibrated by the manufacturer. Commercially available devices often rely upon surface contact being enough to achieve a satisfactory measurement, and so are not destructive in nature.

4.3 Proxy Materials

A technique used by some practitioners is to insert sampling materials, which are assumed to be in hydrophilic contact with the building element to be monitored. This can be achieved through the introduction of new materials (often wooden dowels are used), or alternatively by removing a core from the building material and reinstating it in such a way that it can be removed periodically for assessment.[30] These approaches may use periodic weighing of the insert to assess the relative moisture content of the building fabric. The insert may require several days to reach equilibrium with the fabric. Where inserts are used with different moisture transport characteristics to the material under investigation, for example wooden dowels in stonework, the results cannot be related to the absolute moisture content and may indicate only whether the fabric is getting wetter or drier. The technique is suitable for assessing long term trends, for example the recovery after a flood, or the monitoring of particularly sensitive buildings.

[29] Fridh, L; Eliasson, L; Bergström, D, 2018, "Precision and accuracy in moisture content determination of wood fuel chips using a handheld electric capacitance moisture meter", Silva Fennica. Volume 52, Issue 5, p. 1.

[30] Newman AJ. The independent core method - a new technique for the determination of moisture content. Building Science 1974; 9: 309–313.

Depending on the nature of the proxy material, the method can be either destructive if a core is used, or minimally invasive if a dowel type material is placed with good contact with a surface.

4.4 Environmental Monitoring

If direct measurement of the moisture content of a material is not possible, it is often the practice to measure the relative humidity at the material's surface. The moisture content can be inferred from this as it is related to the relative humidity by the sorption isotherm (a physical characteristic of the material).[31] However, for some materials there can be significant hysteresis between the wetting and drying behavior. At best, environmental monitoring gives an indication of the condition of the material and is most suited to long term monitoring of the building fabric to identify whether it is drying, wetting or has reached equilibrium. A practical application of this is in the monitoring of buildings to identify whether an existing problem has been successfully treated. Commercially available equipment allows multiple sensors to be monitored for extended periods of time to enable a longer-term picture of behavior to be obtained. Proper interpretation of the results from this approach requires experience. This technique is purely non-destructive in nature and is therefore of interest for use in conservation sensitive applications.

[31] Huw Lloyd, technical director, Dr Jagjit Singh, "Environmental monitoring: inspection, investigative monitoring techniques for historic buildings and case studies - brief paper" Environmental Building Solutions Ltd, UK

4.5 Other Techniques

There are a range of additional techniques for measuring moisture content which have been considered for use worldwide but are not currently typical practice. Ground penetrating radar (GPR) has been used to examine the moisture content of building substructures,[32] however, this requires very accurate knowledge of the existing structure to obtain a basic measurement of moisture content. Microwave absorption systems have been examined in the 1960s and 1970s,[33] however, such systems require the alignment of a transmitter on one side of the wall and a receiver on the other side to get a reading, and this is generally impractical for building investigations. Recently work has been undertaken to develop a portable version of a research tool using Nuclear Magnetic Resonance (NMR)[34] which could be used for building investigations. However, the complexity and cost of such devices makes them inaccessible to all but the most specialized of building professionals.

Compared with these methods mentioned, the radio frequency methods such as RFID and IRT are relatively more mature and have great potential to be applied to moisture content measurement for historic buildings. In this thesis, RFID and IRT will be

[32] Dill MJ. A review of testing for moisture in building elements. Construction Industry Research and Information Association, London, 2000.
[33] Watson A. Measurement and control of moisture content by microwave absorption. Build Int 1970; 3(3): 47–50.
[34] Eidmann G, Savelsberg R, Blu¨mler P, Blu¨mich B. The NMR mouse, a mobile universal surface explorer. Journal of Magnetic Resonance Series A 1996; 122: 104–109.

studied and tested as alternate, non/low-destructive techniques to quantitatively measure the moisture content of adobe walls.

Table 4.1: Advantages and disadvantages of common site measurement techniques

Technique	Intervention needed	Type of measurement	Comments
Extractive techniques	Requires hole to be drilled for each measurement.	Absolute moisture content measurements possible; Can measure profiles	uncertainty in the sample extracting process; Allows chemical analysis.
Electrical techniques	Non-destructive, usually surface contact only.	Measures surface (or near surface) conditions; Rapid measurements possible. Relative moisture content measurements only, unless calibrated.	Contact problems with some materials; Presence of salts, metallic or magnetic materials near measurement point can cause errors.
Proxy materials	Can be destructive (cores used) or non-destructive (materials placed in surface contact).	Allows monitoring of long-term trends of the relative moisture content; Instant readings are not possible; Measurement limited to point of contact between proxy material and the substrate.	Unsuitable for monitoring rapidly fluctuating materials; Sampling material can deteriorate; Minimal equipment needed between readings.

Chapter 5 : Infrared Thermography(IRT) and Radio Frequency Identification (RFID) for Recognizing Moisture Anomalies in Building Diagnostics

Accurate quantitative measurement for moisture content has generally required localized sampling and laboratory testing using gravimetric analysis. Other less invasive methods measure moisture content levels in-situ with non-destructive or moderately destructive techniques. Localized quantitative embedded methods use conductance or resistivity measurements. However, these methods can be effective but are subject to localized conditions such as interference from salts and are best used in large numbers to diagnose wall moisture patterns. RFID and Infrared thermography techniques both offer an alternative semi-quantitative, minimally invasive measurement of moisture content compared to direct gravimetric methods. Compared with embedded or extracted quantitative sample analysis, IRT and RFID moisture sensors are relatively inexpensive, easy to use, and provide large scale moisture patterns.

5.1 Infrared Thermography

All objects radiate energy in many wavelengths. Part of that energy can be detected by infrared sensors. If you combine tens of thousands of infrared sensors into a single chip, you can recode all their signals as varying intensities of visible light. The combined and recoded signals are then assembled into a video image which shows a pattern of surface temperatures. Often, these patterns are caused by differences in

moisture content. To understand how thermal imaging relates to building inspections, it helps to understand some characteristics of infrared waves and their behavior in air. [35]

Gamma rays and x-rays have a short wavelength while radio and TV waves have very long wavelengths. Human eyes function in a narrow slice near the middle of the spectrum. We only see wavelengths between about 0.4 and 0.78 microns. (400 to 780 nanometers). Infrared waves are much longer and lower in frequency than visible light—they vary from 1.0 to 24.0 microns in length. Within the infrared band, the waves most useful for examining thermal patterns in buildings are those between 7 and 14 microns in length. These make up a large portion of the heat emissions from surfaces which have near-ambient temperatures. Also, the gasses which make up air—nitrogen, oxygen and water vapor—do not absorb too much of the energy carried by these wavelengths. Therefore, these 7 to 14-micron waves can travel from a surface through the air to the sensor without much interference. Finally, the amount of energy emitted in this range of wavelengths has a very strong dependence on temperature. In other words, small differences in surface temperatures generate large differences in the amount of infrared energy that the surface emits.[36]

Therefore, the 7 to 14 micron infrared signal can indicate small temperature differences and can be used as a sensitive remote sensing technique for quick periodic inspections to detect moisture and other features related to temperature, including

[35] Lewis G. Harriman III, "Practical Aspects of Locating and Measuring Moisture in Buildings"
[36] Kruse, Paul W. "Uncooled Thermal Imaging: Arrays, Systems and Applications". 2001. SPIE Press, Bellingham, WA. www.spie.org

heat losses, missing or damaged thermal insulation in walls and roofs, thermal bridges or air leakage.[37] Much literature can be found making use of thermal imaging to perform different performance analysese of buildings and there are many studies focused on monitoring and conservation of ancient buildings.[38]

Sir Frederick William Hershel discovered the infrared spectrumin 1800. Short-wave infrared (1-3 micrometers) scanners were developed in the late 1940' s to 1960' s; an instantaneous thermal imager was introduced in 1963 by AGA Thermovision, and the first commercial infrared focal plane array (IRFPA) camera was introduced in 1989 by Mitsubishi. In the early 1990' s, computer software was developed to process data collected by the thermal sensors. Portable long wave (8-14 micrometers) infrared focal plane array cameras became available in the mid 1990's.[39] Since then, it has been a valuable tool for building diagnostics. In the field of conservation, infrared thermography exists as a nondestructive tool for detecting moisture patterns in historic structures. Over the years, leading industrial electrical instrument manufacturers such as Fluke and FLIR have produced increasingly higher resolution, lower cost, portable infrared thermal imaging cameras for diagnosing

[37] Balaras CA, Argiriou AA. Infrared thermography for building diagnostics. Energy Build 2002;34(2):171–83.
[38] Avdelidis NP, Moropoulou A. Applications of infrared thermography for the investigation of historic structures. J Cultural Heritage 2004;5(1):119–27.
[39] 6 Herbert Kaplan, Practical Applications of Infrared Thermal Sensing and Imaging Equipment, (Bellingham, Washington: Society of Photo-Optical Instrumentation Engineers, 2007), p. 6.

structures in the field. Publications of successes and limitations of infrared thermography serve as a foundation for exploring potential advancements in the field.[40]

Figure 5.1 : Flir E60 infrared camera. Image from FLIR website

The infrared camera can detect small differences in surface temperatures by receiving the different amount of infrared energy that the surface emits. However, first we need to know out how the moisture content interacts with the surface temperature patterns. Basically, excess moisture creates surface temperature differences in five ways. The first is the most common and most visually apparent in water damage situations:

[40] Domenica Paoletti, et al, "Preventive Thermographic Diagnosis of Historical Buildings for Consolidation," Journal of Cultural Heritage Vol, 14 (2013), pp. 116-121.

① Evaporation. Moisture cools the surface as it evaporates, so that moist areas appear cooler than dry areas which will create a darker (slightly cooler) pattern in the moist areas.

② Thermal lag. Water is dense, so it slows the thermal change of a porous material when ambient temperatures change. Moist areas appear cooler when the rest of the surface is warming up, or warmer when the rest of the surface is cooling down.

③ Differences in thermal conductivity. Moisture increases the density and therefore increases the heat flow through porous materials. Moist areas appear warmer than dry areas on the cooler side of the wall, and cooler than dry areas on the warmer side of the wall.

④ Conduction. Water cools or warms a surface by direct contact when water is flowing, dripping or moving by capillary suction away from a warm or cold source.

⑤ Radiation. If warm or cold water is present inside a wall, the outer surface of that wall can be changed as it absorbs heat from or releases heat to the internal water by radiation.

All these processes are happening at the same time in any building. But evaporative cooling usually dominates thermal images of moisture after a flood, fire or other water event, especially after the building has been stabilized and the source of the water eliminated. Because evaporating moisture always makes a surface cooler, moist

materials indoors (away from the exterior wall) nearly always appear darker - colder - than the surrounding dry material. That's why, in catastrophic water damage situations, infrared cameras have become so popular. They are easy to use, and the images are easy to interpret correctly, which lets professionals proceed with speed and certainty which is not possible with other measurement systems. With the more subtle and complex paths of moisture typical of non-catastrophic investigations, the cameras are still very useful, but such simple interpretation is seldom possible. However, as one looks at the images shown here, it is important to keep in mind that thermal cameras do not see moisture, nor do they actually "see inside the wall." They only show differences in surface temperature. To make an infrared camera useful for moisture inspection, the inspector must be able to interpret the origin of the thermal differences it shows.

Infrared thermography can be a non-destructive tool for detecting moisture patterns for most historic structures, but there remains a need to explore the extent to which infrared thermography can quantitively describe moisture in an adobe wall. By combining knowledge of the fundamentals of construction, evaporation, and relative humidity, this tool can be considered for quantifying moisture content levels in adobe walls.

5.2 Radio Frequency Identification (RFID) Technique

Radio-frequency identification (RFID) uses electromagnetic fields to automatically identify and track tags attached to objects. There are two types of RFID

tags. Passive tags are powered by energy from the RFID reader's interrogating radio waves. Active tags are powered by a battery and thus can be read at a greater range from the RFID reader. Compared with active tags, passive tags are more wildly used due to their lower cost, better portability and sacrificial nature. The tag can be embedded and left in walls for long-term monitoring.

In 1983, the first patent to be associated with the abbreviation RFID was granted to Charles Walton.[41] Since then, RFID technology has officially entered the civilian business era.

With the growing demands and rapid development of communication technology, research on integrating sensors with RFID tags has gained interest. Embedding sensor elements in RFID tags reduces the cost of setting up a sensor system but also paves the way for various applications of RFID to be deployed. RFID-based sensors are used in various applications from food items to seepage detection, and from crop health monitoring to pharmaceutical tracking. In the food industry, RFID sensors have been used to detect the moisture level in shelled peanuts.[42] For building diagnosis, RFID sensors can be embedded in walls. In moist surroundings, the difference in the backscattered received signal yields degradation in terms of dielectric losses.[43] Besides other applications, RFID tags are used in the field of agriculture. Inkjet-printed RFID tags

[41] Charles A. Walton "Portable radio frequency emitting identifier" U.S. Patent 4,384,288
[42] TRABELSI, S., NELSON, S. O. “Microwave sensing method for simultaneous and independent determination of bulk density and moisture content of shelled peanuts”. IEEE Antennas and Propagation Society International Symposium, 2006, p. 3187–3190.
[43] SIDEN, J., ZENG, X., UNANDER, T., et al. Remote moisture sensing utilizing ordinary RFID tags. Proceedings of IEEE Sensors, 2007, p. 308–311

based on the paper substrate can be used for monitoring soil moisture.[44] RFID sensors are used as much in the field of medicine as they are in any other field. Within the scope of medicinal application, the moisture level of a patient's wound can be readily monitored using RFID tags.

For building diagnosis, in situ monitoring of moisture content in existing walls has been a challenge. There are still few reliable, validated methods to seamlessly integrate monitoring with cyclical maintenance that is not prohibitively destructive. For earthen materials which are more vulnerable to destructive techniques, the task is more

Figure 5.2: UHF RFID handheld sled reader and RFID tags. image from onvergence Systems Limited website and smartrac website.

challenging. At this point, RFID entered the professionals' vision as an alternative technique for long-term moisture monitoring that was limited in destructiveness, low-

[44] KIM, S., LE, T., TENTZERIS, M. M., et al. An RFID-enabled inkjet-printed soil moisture sensor on paper for 'smart' agricultural applications. Proceedings of IEEE sensors, 2014, p. 1507–1510

cost and resilient enough to integrate with ongoing maintenance and repair cycles without the need for removal once monitoring was completed.

"The use of RFID tags to measure the moisture content of their surrounding environment is based on the fundamental principle that water has a relatively high dielectric constant between 70 and 80 dbi, meaning it is relatively efficient at storing electrical energy in an electric field. Effectively, the RFID tag is a planar inductor-capacitor circuit. The capacitance of the circuit is increased when the tag's surrounding environment becomes saturated, and the impedance of the tag antenna is matched to reflect this change. These relative changes in the tags' electrical properties are encoded in the backscattered signal and can be used to infer the properties of its surrounding material, or rather changes to these properties over time. The benefits of this method include the ability to transmit data without requiring optical line-of-site or physical contact with the medium being measured."[45]

However, the most significant limitation of this methodology is the sensitivity of the tag near-fields to interference. This interference ideally is the result of moisture in the area surrounding the tag. However, it can also result from other factors. Besides, the reliability of the received signal strength indicator (RSSI) that the RFID reader receives from tags is relatively low. These limitations may make professionals doubt whether the RFID technique can quantitively measure the moisture content especially in adobe walls.

[45] *Evan Oskierko – Jeznacki, "An Alternative Technique for Low-Cost, Non-Destructive Moisture Monitoring in Adobe Walls using Embedded RFID Technology", Unpublished*

This question frames the research presented here. In this thesis, both RFID and IRT are comparatively tested to quantitatively measure and to monitor moisture content in sand columns.

Chapter 6 : Correlation Tests on Sand Columns

This chapter describes the testing procedure developed to assess the application of RFID and IRT to record moisture levels in adobe walls using surrogate sand columns. The objectives are to:

1. Distinguish different moisture content levels in a controledporous medium.

2. To accurately quantify moisture content values against other direct methods such as gravimetric analysis.

If objective 2 is met, this methodology demonstrates that it is possible for architectural conservators to use infrared thermography and RFID moisture sensors as a nondestructive tool to determine moisture content readings during field investigations centered on moisture in historic adobe structures.

The testing methodology for this thesis employs five sand column samples of known granulometry as surrogate porous bodies for adobe. Sand of known grain size distribution was used to ensure a measure of consistency across samples when comparing the IRT and RFID methods of moisture detection against each other. The sand was packed in plastic containers and RFID tags were embedded into the sample columns at set levels. The surfaces of the samples were scanned with a FLIR E60 infrared camera dry and during wetting until fully saturated at timed intervals to correlate infrared thermograms to the RFID data.

6.1. Material Selection and Characterization Tests

The selected sand type was a commercial builder's sand 'Quikrete' brown play sand, which is a specially graded fine quarzitic sand that has been washed, dried and screened. This sand displays high permeability, high porosity when packed and is easy to dry making it a desirable test medium for this investigation to provide stable calibration data.

Figure 6.1: The brown sand

Characterization test

1. porosity

The apparent density of the brown sand can be calculated by conducting volumetric and gravimetric analyses of a measured sample. The real density of the sample was determined using a fluid displacement method. The apparent and real densities of each sample were compared to determine the porosity of various granular beds.

After testing, the apparent density (ρ_a) is:

$$\rho_a = \frac{M_S}{V_a} = 1.416 \times 10^3\ kg/m^3$$

the real density (ρ_r) is:

$$\rho_r = \frac{M_S}{V_r} = 2.622 \times 10^3 kg/m^3$$

Therefore, the porosity (ε) and percent porosity (%ε) for this sand are:

$$\varepsilon = 1 - \frac{\rho_a}{\rho_r} = 1 - \frac{1.416 \times 10^3}{2.622 \times 10^3} = 0.46$$

$$\%\varepsilon = \left[1 - \frac{\rho_a}{\rho_r}\right] \times 100 = 46\%$$

the porosity of commercially made adobe bricks is around 40%[46], which is close to the sand's porosity 46%.

2. Particle size distribution (granulometry)

Particle size distribution of natural and artificial aggregates such as sand and soil are determined by sieving. The physical properties of sand and soil can be used as a means of classification for comparative purposes and to predict certain physical properties such as porosity, permeability, and capillarity.

In this test, a laboratory vibrating sieve machine was used to continuously sieve the sand material. The vibratory action produced by the power unit moves the sample over the sieve in a unique way producing faster more efficient sieving, while the rapid vertical movements also help to keep the apertures clear from binding.

[46] P Lertwattanaruk, "The Physical and Thermal Properties of Adobe Brick Containing Bagasse for Earth Construction" Thammasat University

Figure 6.3: Sieve machine.

Figure 6.4: Sieve result

Sieve number	Screen size (um)	Msx (g)	%Msx	%Mpt
8	2360	0	0	100
16	1180	1.24	0.1	100
30	600	20.67	1.6	99.9
50	300	456.03	35.2	98.3
100	150	703.99	54.4	63.1
200	75	101.95	7.9	8.7
Pan	1	10.06	0.8	0.8

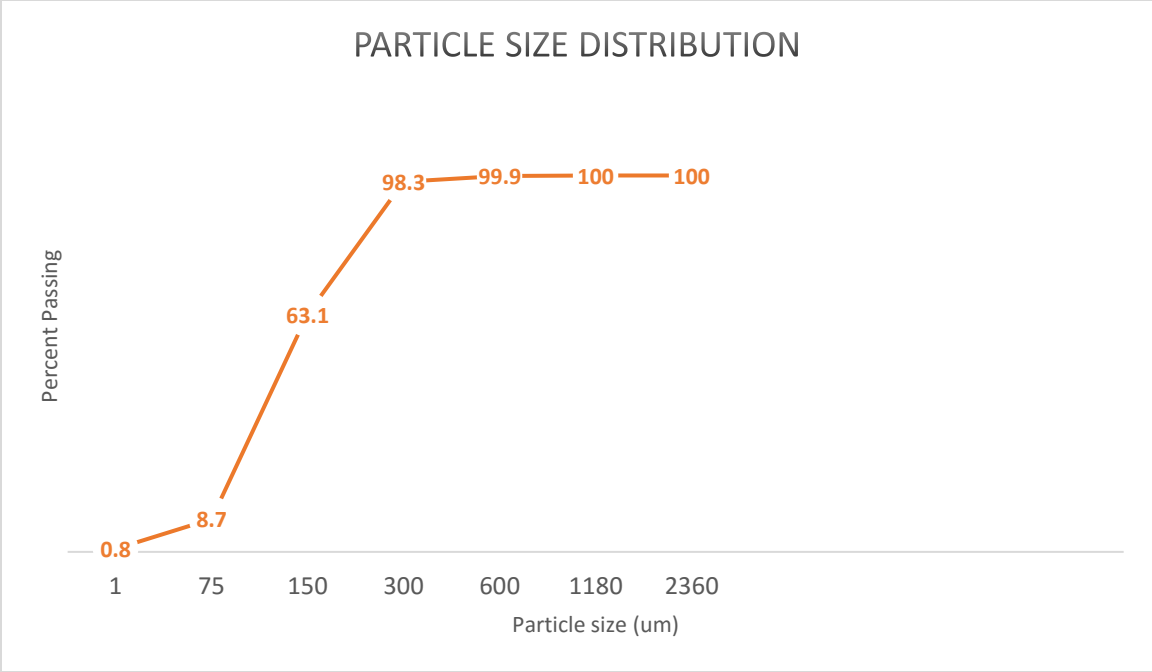

This brown sand is a very fine sand of small grain sizes mainly varying from 150-300 µm. There is almost no grain fraction larger than 600 µm because the passing percentage of the first two sieves are both 100%.

6.2. Preliminary Testing

The signal received from the RFID tags is a function of distance to the reader therefore tag depths had to be known before creating the column samples. To be more specific, if the RFID tags were embedded too deeply from the top surface, the reader

might not read the signal.

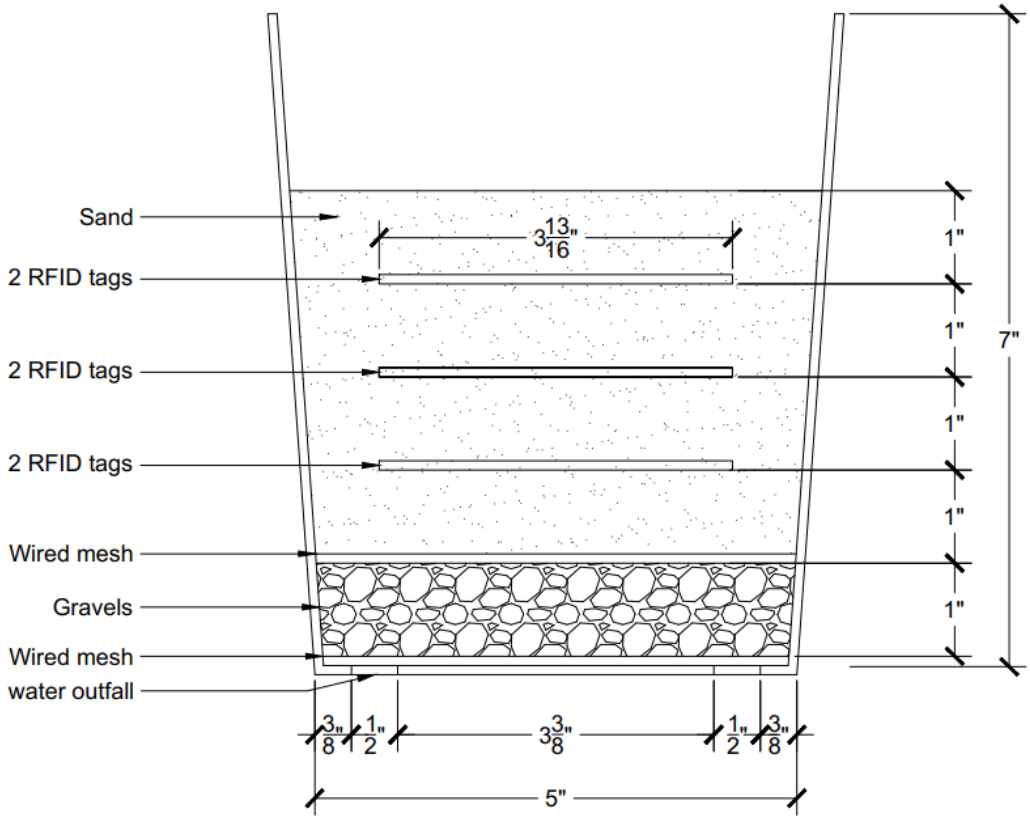

Figure 6.5: the sand column

Figure 6.6 ：insert RFID tags

Therefore, in the preliminary test, RFID tags were embedded at three different depths: 1 inch, 2 inches and 3 inches from the top surface. Before embedment, all tags were renamed and checked to ensure they worked. After assembling the sample, the sample was fully saturated (until water flowed out from the bottom drainage hole). The result showed that the 2 tags at a 3 inch depth could not be read while the tags at 1 and 2 inches were readable. Therefore, tags were placed at a maximum distance of 2” from the top of the sample

6.3. Sample Preparation

Figure 6.7: Test materials

Sample components (from left to right):

1. Quikrete brown play sand.

2. 304 Stainless Steel Woven Mesh Sheet (ASTM E2016-06)

3.Plastic containers

4. Gravel

First, a layer of steel mesh was put on the bottom of the plastic containers to prevent the gravel from flowing from the drainage hole. Afterwards, one-inch of gravel was laid on top of the metal mesh to enhance drainage . Another layer of steel mesh was put on the gravel layer to contain the sand above. Four inches of sand was then laid on the top and two RFID tags were embedded two inches from the top). The containers were tapped repeatedly to insure uniform compaction of the sand. This scheme was designed to produce five samples in the same experiment. One sample was used as a control group (dry) and the others were tested -all wet using IRT, RFID and gravimetric analysis. Because the samples were not completely dry after they were assembled, weighing and labeling the samples was postponed after oven dry for 48 hours.

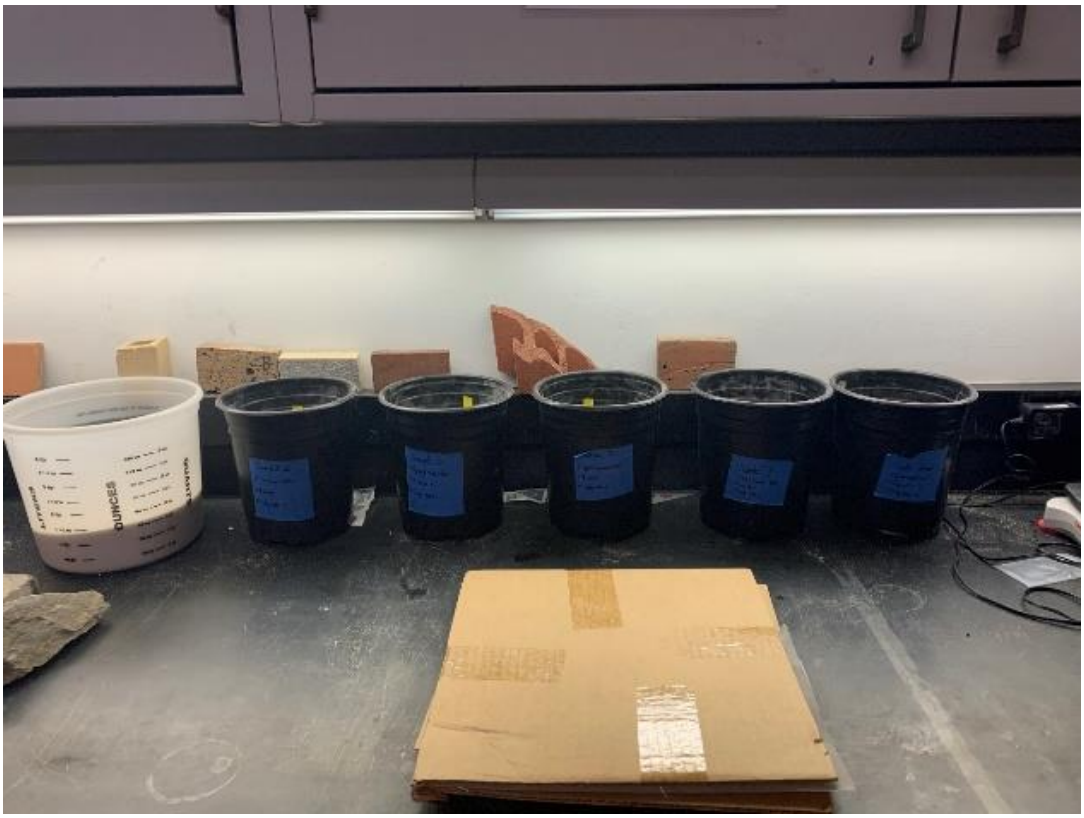

Figure 6.8: five samples

6.4. Monitoring by Infrared Thermography and Gravimetric Analysis

6.4.1 Equipment

A FLIR E60 handheld infrared thermal imager was used throughout this experiment. Specifications for this device include the capability to measure a surface temperature range of -20°C- 650°C (-4°F to +1202°F) at an accuracy of ±2°C or 2% at ambient temperature 10°C to 35°C (+50°F to 95°F). Operating ambient temperature ranges were from –15°C to +50°C (+5°F to +122°F). The thermal imager includes a 320x240 focal plane array and an uncooled microbolometer detector type that measures an infrared spectral band of 7.5 µm - 13 µm. For this procedure, the emissivity value for the camera was set to 0.85 for common. This camera includes a

Picture-in-Picture capability that allows for the camera to produce a thermal image over a visible-light image. The camera was mounted on a ladder to hold the handheld device at a fixed height. For this thesis, only the infrared images were of concern, so the camera was positioned at maximum adjacency to the sample to minimize the effects of background noise. Samples were placed on a white stacking shelf. This set up allowed for each thermal image of a sample to be captured in the same place for all rounds of testing.

The RFID reader used in this experiment was a CS108 Convergence Systems Limited sled handheld reader which is the longest read range UHF RFID handheld sled reader in the world. The read range of this reader is up to 20 meters with linear polarized antenna (tag and environment dependent) and the frequency range is 902-928 MHz. The accuracy of the signal strength the reader receives is unknown but from the preliminary test, the accuracy is not high, and the received signal was easily affected by the environment. Operating ambient temperature ranges were from –20°C to +55°C (-4°F to +131°F). The reader works with all Android phones or iPhones, so the data can be viewedon phone and real-time transmitted to a laptop.

The tags used were manufactured by Smartrac® and are classified as EPC Class 1 Gen 2, a UHF wireless communication standard. All tags in this class can communicate with any commercially available transceiver of the same class. The tags measure approximately 3.8” by 1.1”.

Figure 6.9: Test set-up

6.4.2 Test Procedure

All assembled sand columns were placed in a drying oven at 75°C for 48 hours and then weighed with a balance sensitive to 0.01g to obtain the dry weight. After this step, all samples were left at room temperature for 12 hours to allow them to cool to room temperature in case of affecting the infrared result. Then, all samples were

saturated with a water spray. Water was carefully sprayed on the surface of the sample while avoiding disturbance of the sand packing and alteration to the surface texture thus affecting the subsequent thermal infrared image.

While the samples were saturating, an Onset Hobo 12-012 External Temp/RH Data Logger was installed in the testing room to monitor ambient temperature and relative humidity at one-minute intervals. The temperature sensor is limited to an accuracy of ±0.21°C from 0° to 50°C in a temperature range of -20° to 70°C and the RH sensor records a range of 1% to 95% at -40° to 75°C with an accuracy of ±2.5% from 10% to 90%. The clock of the data logger was synchronized to the FLIR E60 for data correlation between room conditions at the time a thermal image was captured. This data logger has a memory capacity of 128KB at one-minute intervals.

After the samples were saturated and water no longer flowed out from the drainage holes, the weight of the samples was measured and the moisture content was calculated by difference between the dry weight and real-time 'wet' weight of the samples, and then the signal strength received by the reader was recorded. Because the signal fluctuated, readings were taken continuously for one minute and the average was recorded.

Samples were next monitored by infrared thermography. With the data logger clock synchronized to the thermal imager clock, real-time room temperature and relative humidity values were recorded.

The infrared camera was allowed ten minutes to warm up before taking a set of readings. Batteries were charged to full before testing to make certain the battery could power the camera throughout each installment of test. For consistency of surface temperature measurements between images, the camera needed to remain powered for the entire interval of testing. Samples were removed from the drying cases and immediately placed onto the shelf to capture a thermal image. Background temperatures were set on the thermal camera according to the room temperature. All images were recorded as a JPG file and imported into FLIR TOOL software for data analysis. All thermal images within a testing round were registered to a uniform surface temperature scale to allow visual comparison of the images. This process was repeated at eight different drying intervals and was repeated twice for each assembly to compare data.

Figure 6.10: samples in drying cases.

Chapter 7: Test Results and Analysis

7.1. Thermal Images

For consistency across samples, all samples were conditioned in the same manner and placed in the same room environment. The sample center point temperature was chosen for analysis because it is most representative of the overall surface temperature. In the thermal images, the temperature of the edges of the sample appears to be higher than the center, which may be attributed to more rapid drying at the edges. Thermal images were taken between 3/12/20 to 3/16/20 which resulted in 8 sets of data for room conditions that ranged from 68.51°F- 70.28°F and 20.88%- 52.54%RH. Starting from March 12th, 2020, average surface temperatures of the samples were measured with the infrared camera. Moisture contents were obtained by gravimetric analysis for later study to assess the relationship between the measured moisture content, surface temperature, and ambient conditions.

The second round of tests started on 20th March. Thermal images were taken between 3/20/20 to 3/26/20 which resulted in 8 sets of data for room conditions that ranged from 75.89°F- 80.58°F and 21.73%- 47.88%RH. Due to the outbreak of COVID-19, the university and laboratory were shut down. Therefore, the second-round of tests was done at another location with different environmental conditions with the first test.

The environmental temperature and RH% between 03/12/2020 to 03/16/2020

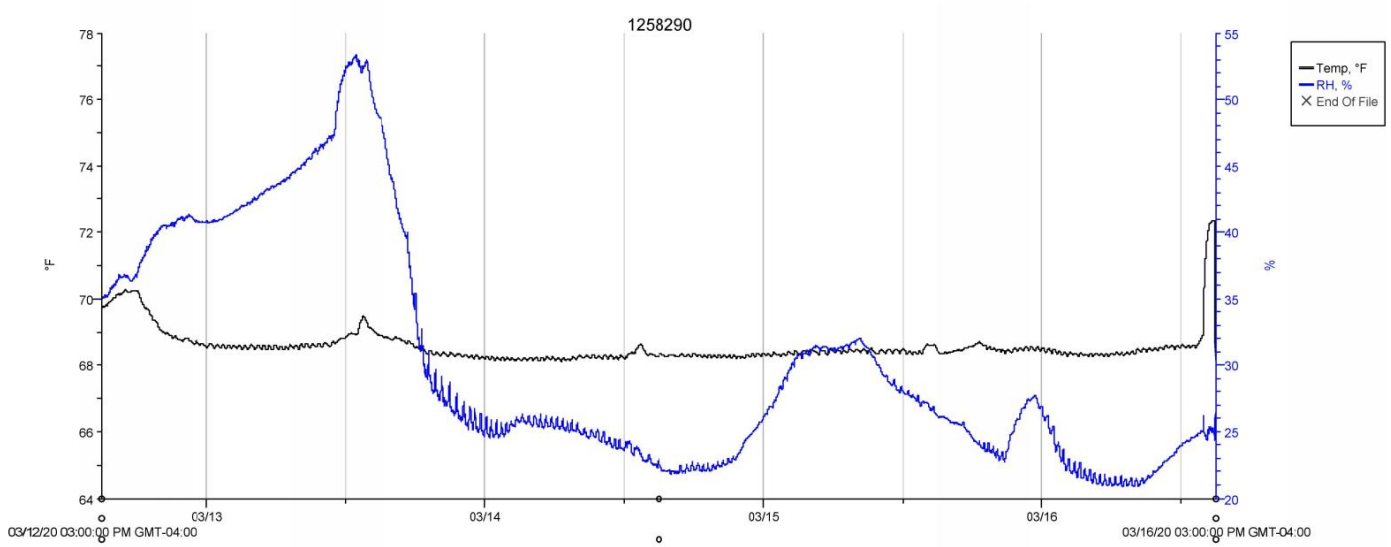

The environmental temperature and RH% between 03/20/2020 to 03/26/2020

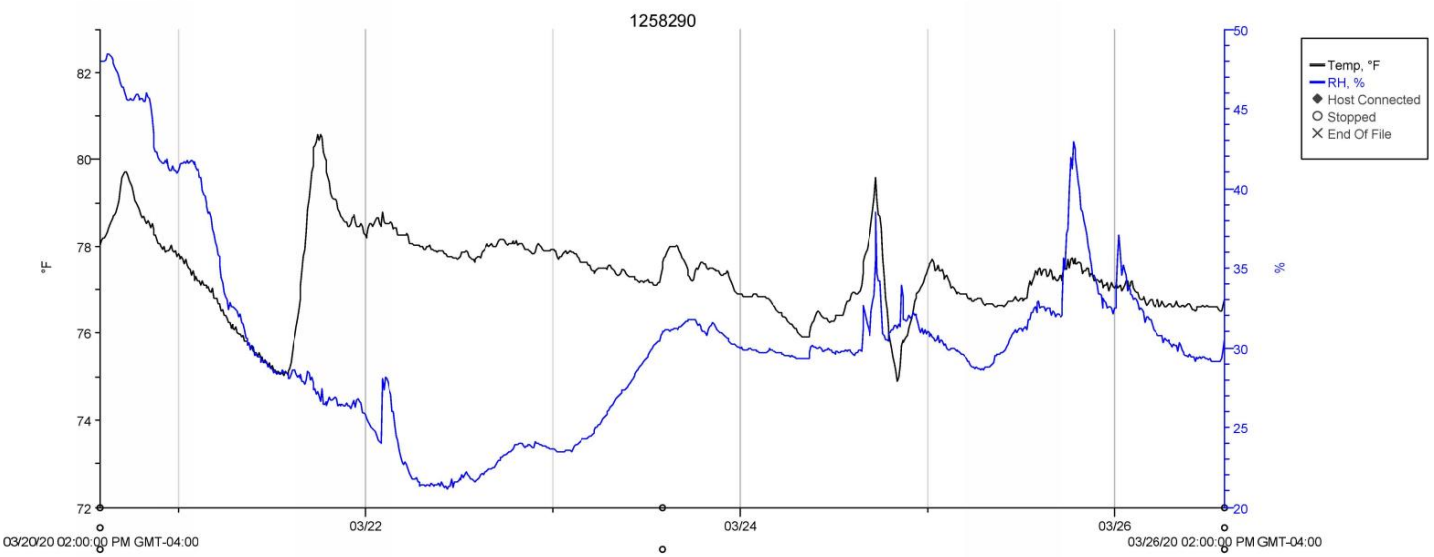

Thermal Images

Date: 03/12 – 03/16

	0 min	30 mins	1h	2h	1st day	2nd day	3rd day	4th day
Control group (Dry)	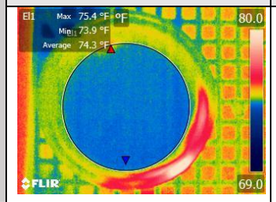	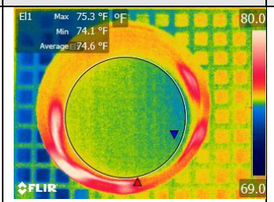	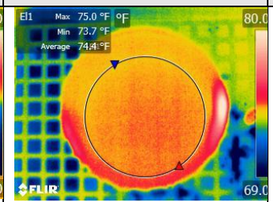	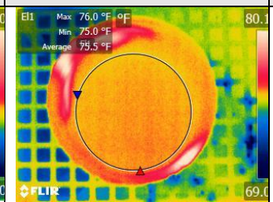	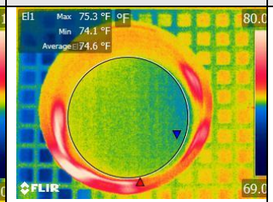	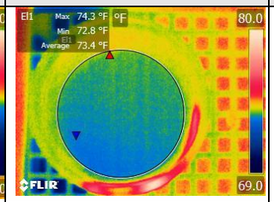	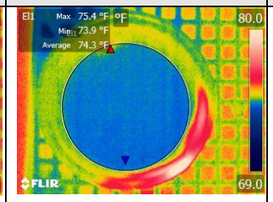	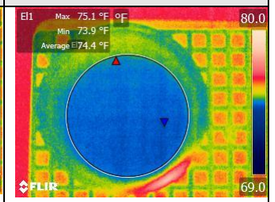
Group 1	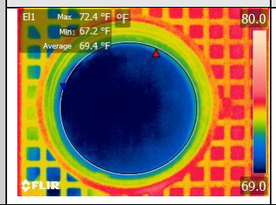	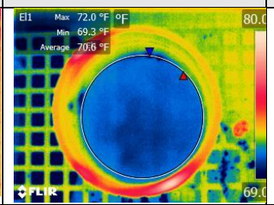	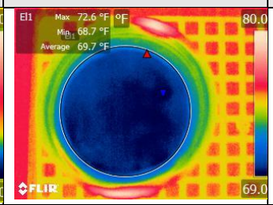	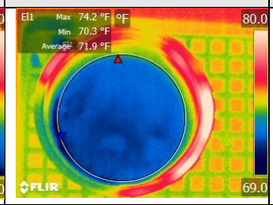	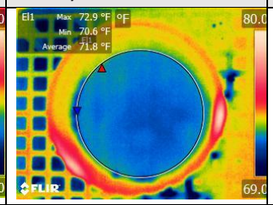	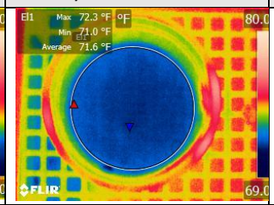	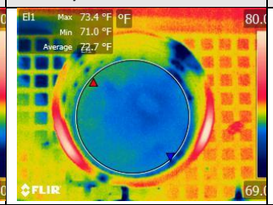	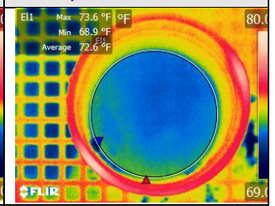
Group 2	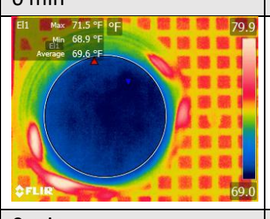	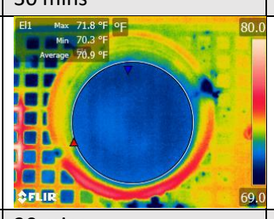	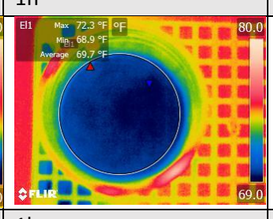	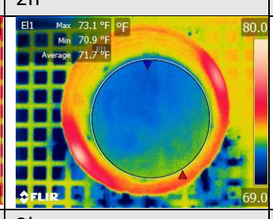	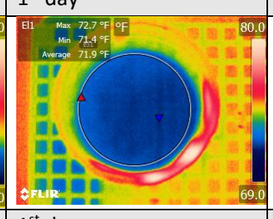	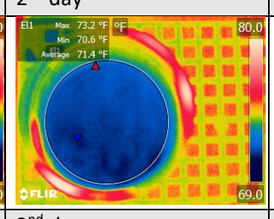	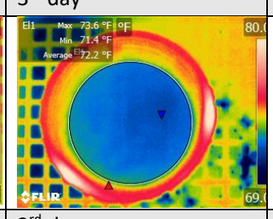	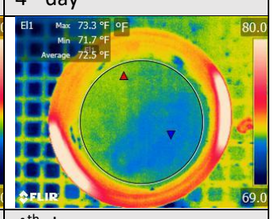
Group 3	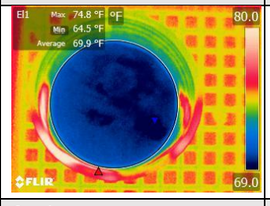	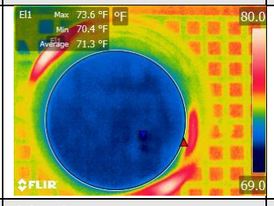	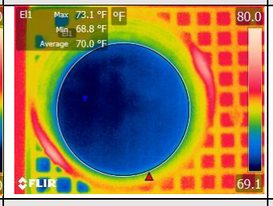	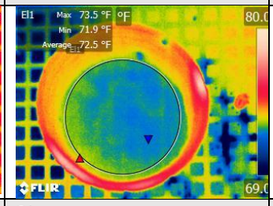	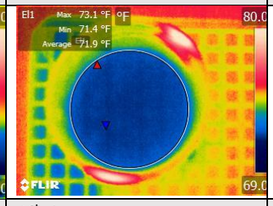	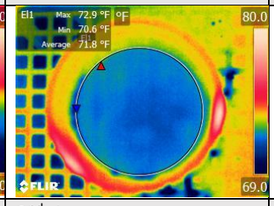	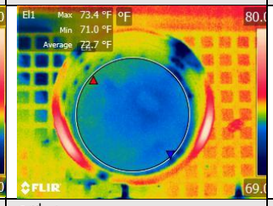	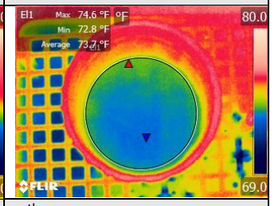
Group 4	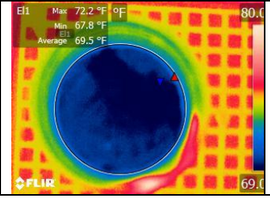	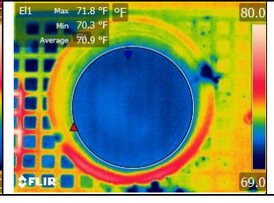	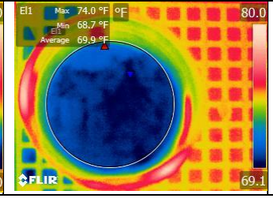	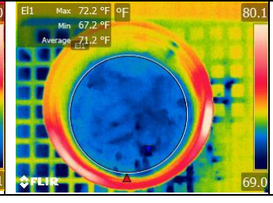	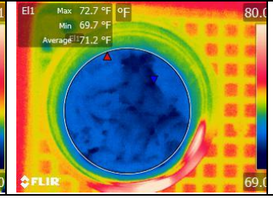	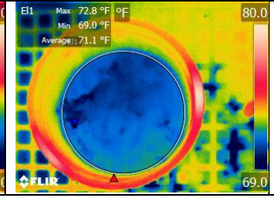	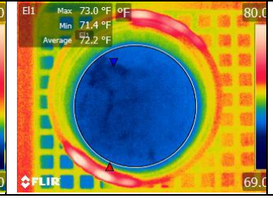	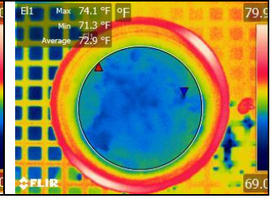

Thermal Images

Date: 03/20 – 03/26

	0 min	1h	12h	24h	2nd day	3rd day	5th day	7th day
Control group (Dry)	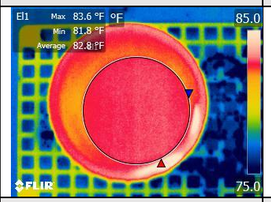	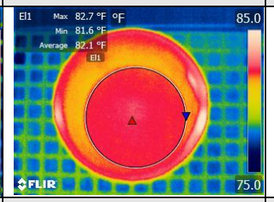	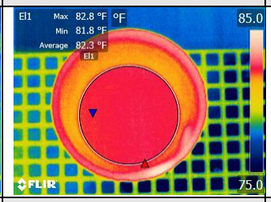	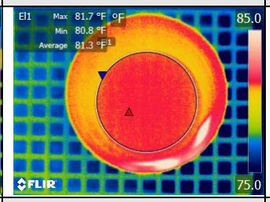	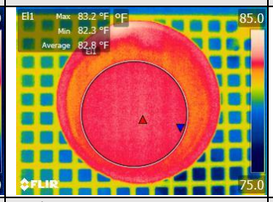	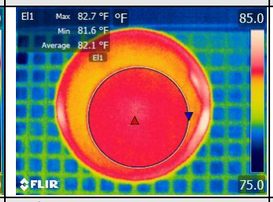	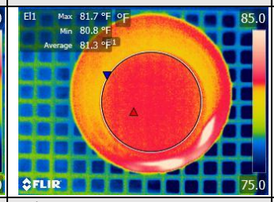	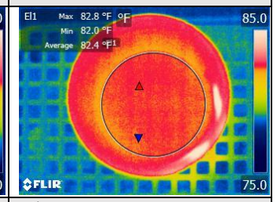
Group 1	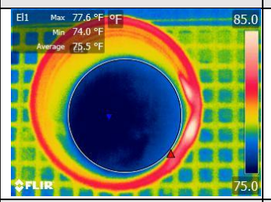	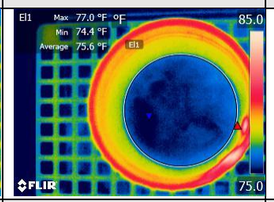	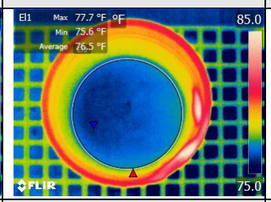	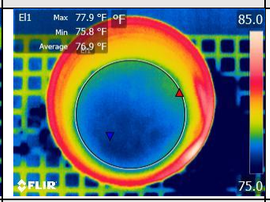	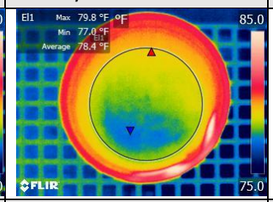	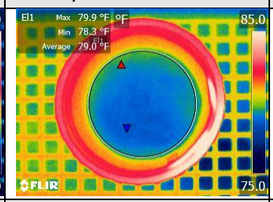	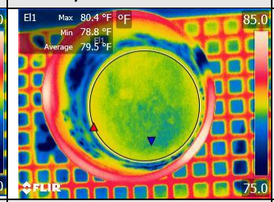	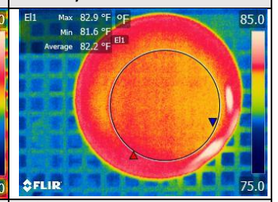
Group 2	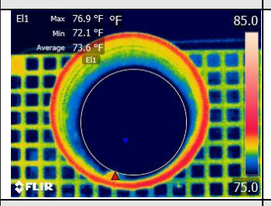	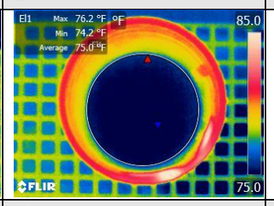	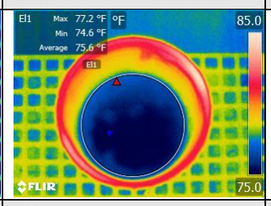	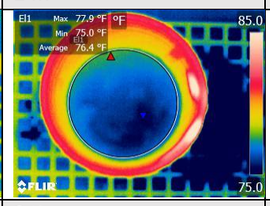	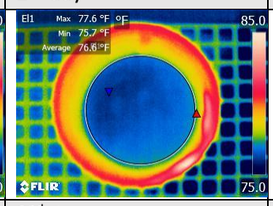	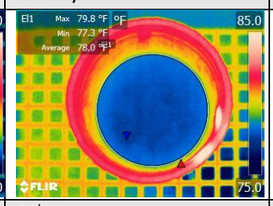	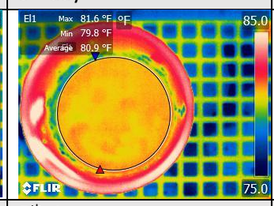	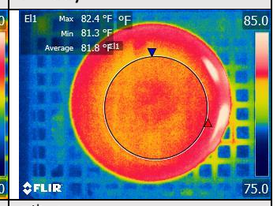
Group 3	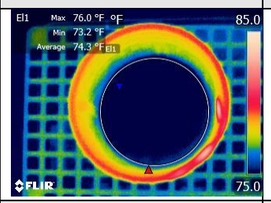	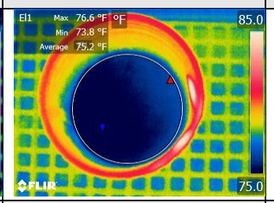	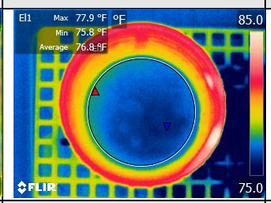	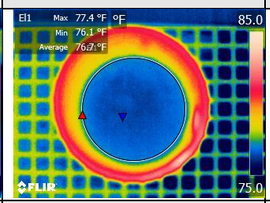	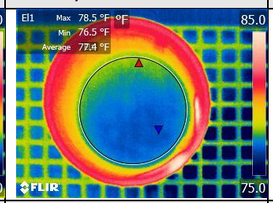	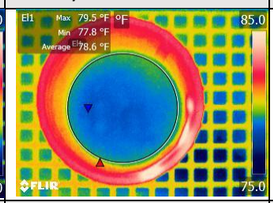	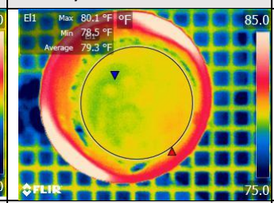	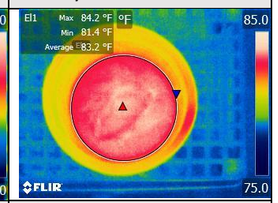
Group 4	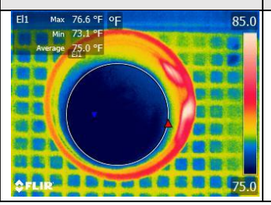	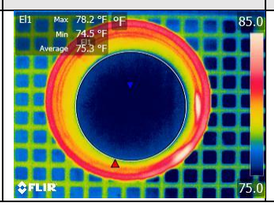	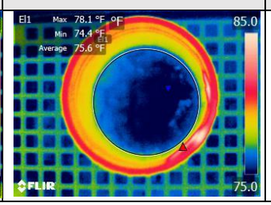	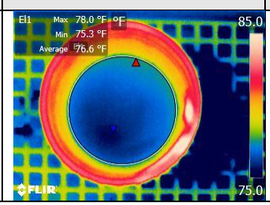	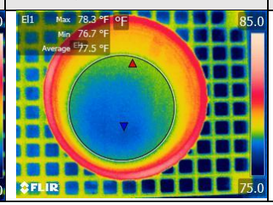	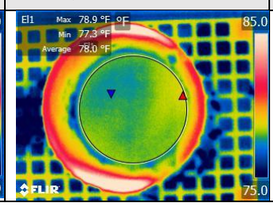	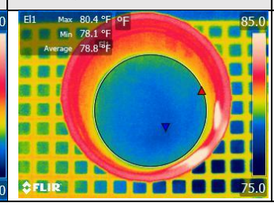	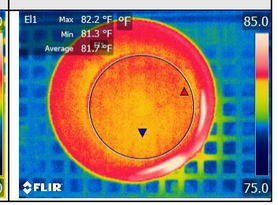

7.2. RFID results

The 1st round of tests (received signal strength dbi):

	0 mins	30 mins	1 h	2 h	24 h	2nd day	3rd day	4th day
Control Group	-39/-42	-38/-40	-41/-43	-41/-43	-40/-43	-40/-43	-41/-45	-41/-44
Group 1	-53/-70	-52/-67	-53/-63	-50/-53	-51/-53	-49/-50	-47/-49	-45/-47
Group 2	-46/-67	-47/-68	-52/-66	-46/-52	-49/-52	-49/-53	-45/-50	-45/-47
Group 3	-50/-64	-54/-55	-55/-55	-53/-55	-52/-54	-51/-53	-50/-53	-48/-52
Group 4	-53/-69	-53/-67	-50/-66	-51/-65	-55/-64	-54/-59	-52/-60	-47/-56

The 2nd round of test (received signal strength dbi):

	0 mins	1 h	12 h	24 h	2nd day	3rd day	5th day	7th day
Control Group	-52/-54	-54/-55	-52/-53	-53/-54	-53/-54	-53/-54	-51/-53	-52/-54
Group 1	-65/-68	-70/-72	-62/-68	-59/-63	-58/-61	-56/-60	-54/-59	-53/-55
Group 2	-69/-71	-69/-70	-58/-73	-54/-67	-50/-67	-47/-65	-50/-61	-49/-50
Group 3	-71/-72	-62/-68	-61/-65	-58/-66	-56/-63	-49/-60	-51/-56	-52/-55
Group 4	-69/-72	-70/-75	-69/-71	-65/-69	-64/-66	-61/-63	-52/-56	-50/-53

7.3. Gravimetric analysis result

The 1st round of tests(g):

	0 mins	30 mins	1 h	2 h	24 h	2nd day	3rd day	4th day
M cg	1698.2	1698.2	1698.2	1698.2	1698.1	1698.1	1698.1	1698.2
MC cg(%)	0.27	0.27	0.27	0.27	0.26	0.26	0.26	0.27
M1	2071.4	2064.5	2054.4	2045.5	2030.4	1975.4	1970.1	1939.6
MC1(%)	24.39	24.06	23.57	23.13	22.37	19.47	19.18	17.47
M2	2108.1	2098.4	2097.8	2096.7	2082.1	2035.4	2031.3	2001.6
MC2(%)	23.64	23.17	23.14	23.09	22.38	20.02	19.81	18.22
M3	2134.3	2131.1	2129.5	2128.1	2112.5	2067.1	2062.4	2029.2
MC3(%)	23.33	23.18	23.11	23.04	22.29	20.04	19.80	18.06
M4	2001.5	1995.6	1995.1	1994.6	1979.7	1935.3	1930.2	1897.5
MC4(%)	22.74	22.44	22.41	22.39	21.61	19.18	18.89	16.99

The 2nd round of tests(g):

	0 mins	1 h	12 h	24 h	2nd day	3rd day	5th day	7th day
M cg	1119.3	1120.7	1120.7	1122.1	1122.8	1123.1	1123.1	1123.3
MCcg(%)	0.12	0.40	0.40	0.68	0.81	0.87	0.87	0.91
M1	1236.7	1233.2	1212.1	1200.1	1178.8	1121.3	1071.6	1059.5
MC1(%)	26.48	26.10	23.72	22.30	19.64	11.46	2.91	0.58
M2	1314.2	1310.8	1287.9	1280.1	1263.6	1201.7	1149.1	1142.9
MC2(%)	25.82	25.45	22.87	21.95	19.92	11.30	2.37	1.20
M3	1307.6	1304.3	1282.1	1273.1	1250.9	1200.4	1156.3	1118.3
MC3(%)	27.67	27.33	24.90	23.87	21.21	14.40	7.41	0.40
M4	1252.4	1249.6	1241.1	1232.7	1214.2	1154.7	1101.1	1068.2
MC4(%)	27.53	27.23	26.32	25.40	23.28	15.57	7.17	1.13

7.4. Analysis and Conclusions

The purpose of this thesis was to:

1. determine if the infrared camera can determine moisture content levels by measuring temperature, therefore the average surface temperature recorded by the infrared camera was examined by graphical analysis to determine if there was any relationship between moisture content and temperature (Figure 7.4.1, 7.4.2, 7.4.3, 7.4.4).

2. determine if the RFID technique can quantitively measure the moisture content according to the signal strength the RFID reader received, therefore the signal strength recorded by the RFID reader was examined by graphical analysis to determine if there was any relationship between moisture content and received signal strength (Figure 7.4.5, 7.4.6, 7.4.7, 7.4.8).

Analysis 1: Infrared Thermography

Firstly, the relationship between the measured moisture content and the surface temperature (T) was analyzed. Then, the relationship between the measured moisture content and the surface temperature difference (ΔT) between the control group and the other 4 sample groups was analyzed. In Figure 7.4.1, the surface temperature data from the first-round test is presented In Figure 7.4.2 the temperature difference (ΔT) data from the first-round test is presented. When the surface temperature is less than room temperature, evaporative cooling is taking place.

Next, in Figure 7.4.3, the surface temperature data from the second-round test is presented. In Figure 7.4.4 the temperature difference (ΔT) data from the second-round test is presented.

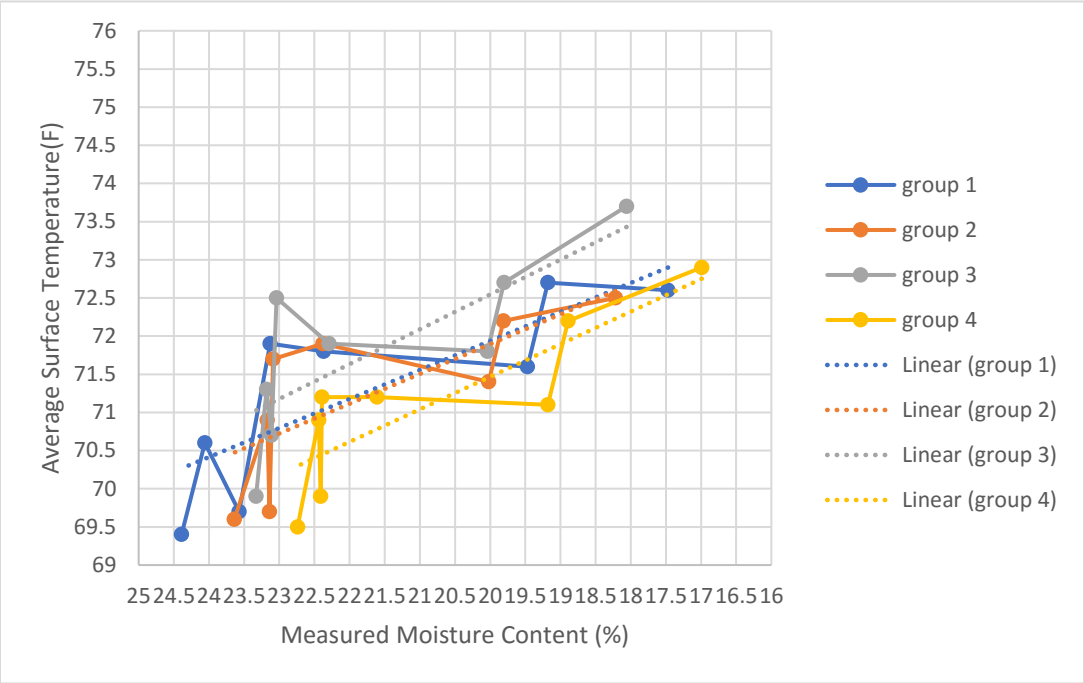

Figure 7.4.1: Graphical analysis of data from 1st-round test

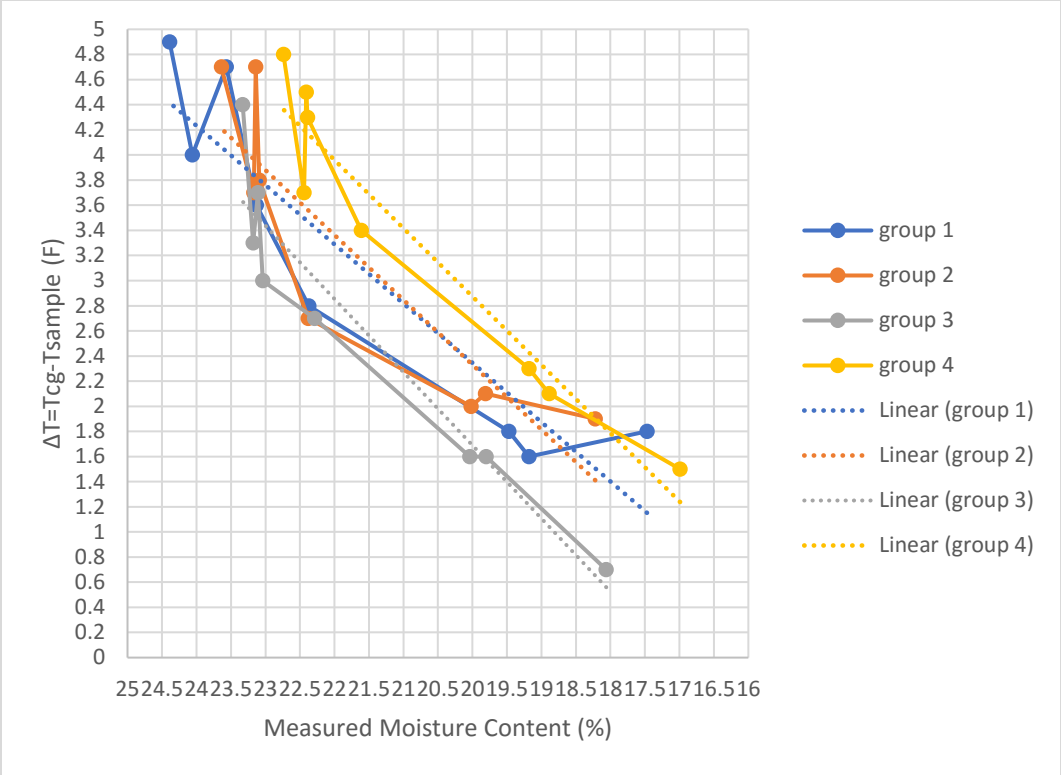

Figure 7.4.2: Graphical analysis of data from the first-round test; The ΔT is the sample surface temperature subtracted from the temperature of control group.

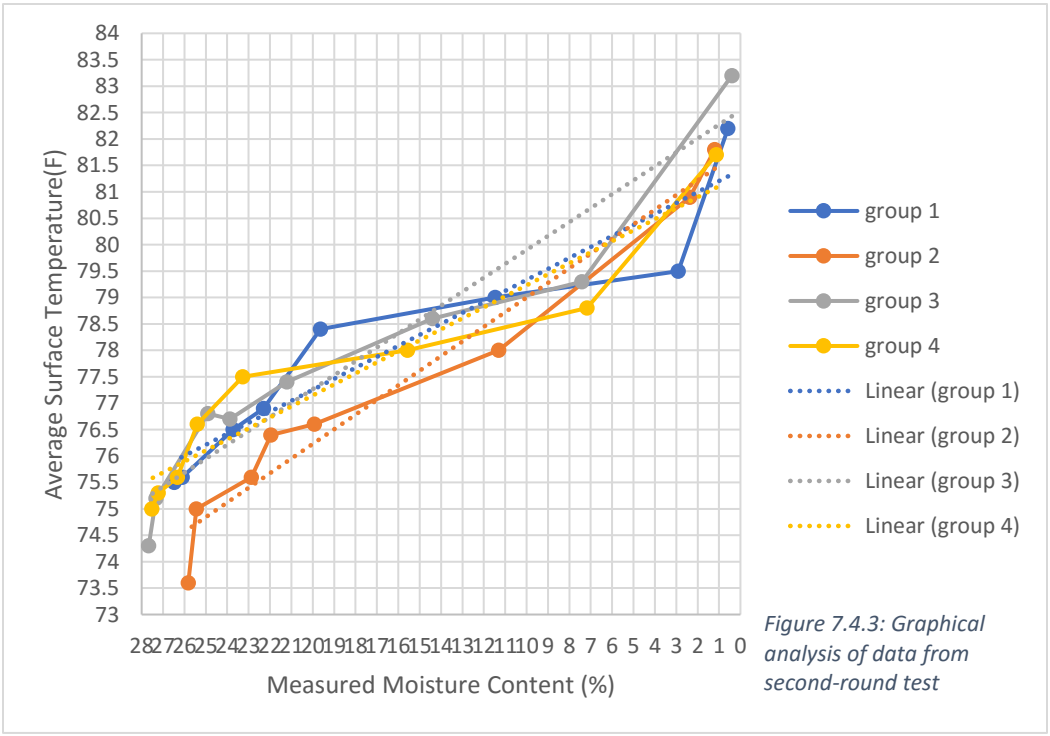

Figure 7.4.3: Graphical analysis of data from second-round test

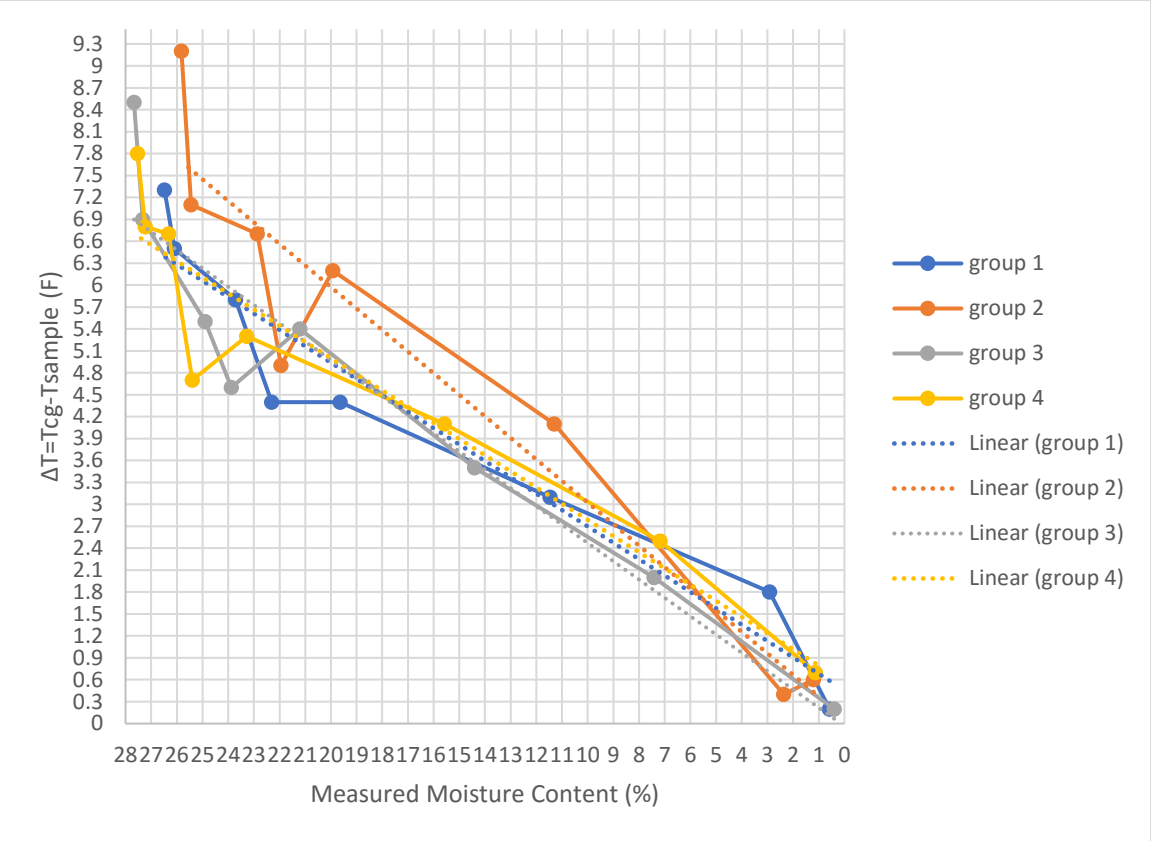

Figure 7.4.4: Graphical analysis of data from the second-round test; The ΔT is the sample surface temperature subtracted from the temperature of control group.

All four groups show a linear relationship between surface temperature and measured moisture content as well as a linear relationship between ΔT (temperature difference between control group and other groups) and moisture content in the two rounds of test. However, the first-round of test appearsto have a more obvious linear relationship and the slopes of the different groups are also closer possibly due to the different test locations (ambient condition).

Analysis 2: RFID technique

The relationship between the measured moisture content and the received signal strength from embedded tags was analyzed. Each sample was embedded with 2 RFID tags. In Figure 7.4.5, the received signal strength data of chip 1 in each sample from the first-round test is presented. In Figure 7.4.6 the received signal strength data of chip 2 from the first-round test is presented. Next, in Figure 7.4.7, the received signal strength data of chip 1 from the second-round test is presented. In Figure 7.4.8 the received signal strength data of chip 1 from the second-round test is presented.

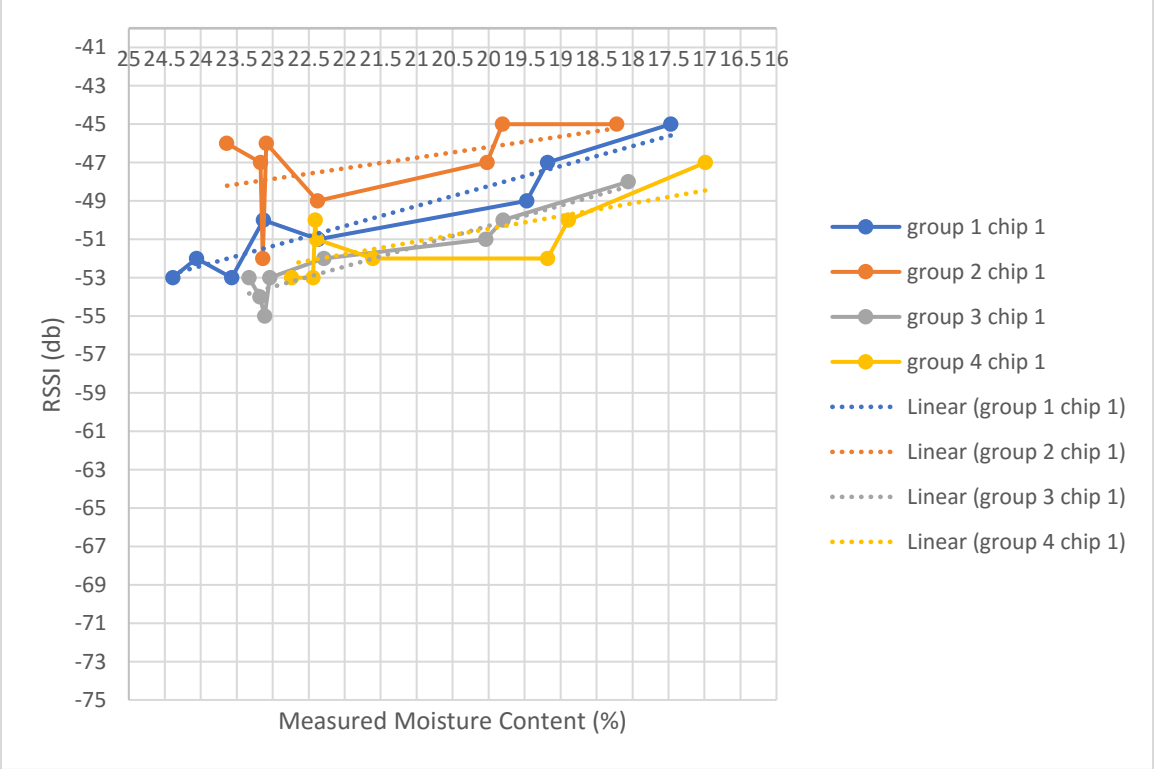

Figure 7.4.5: Graphical analysis of RSSI data of chip 1 from 1st-round test.

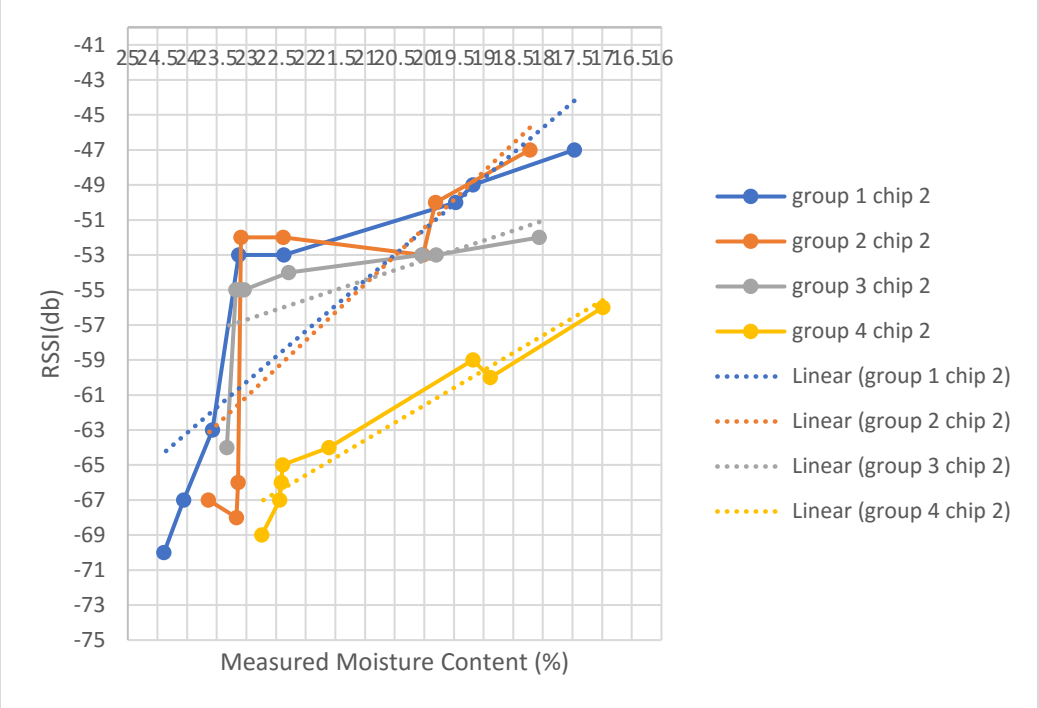

Figure 7.4.6: Graphical analysis of RSSI data of chip 2 from 1st-round test.

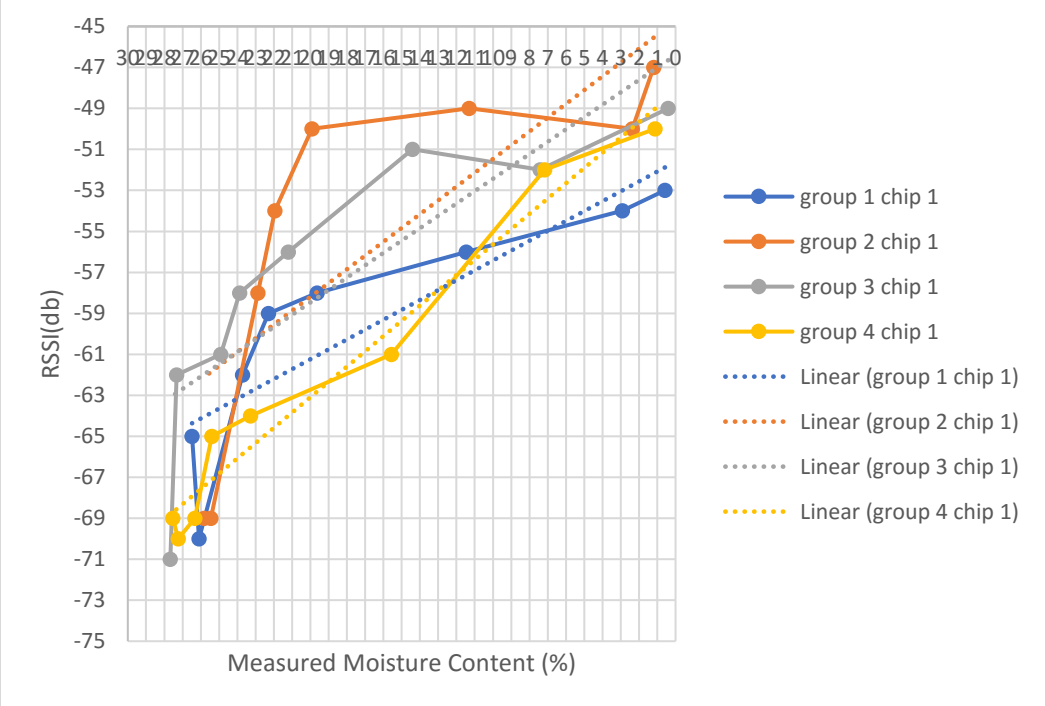

Figure 7.4.7: Graphical analysis of RSSI data of chip 1 from second-round test.

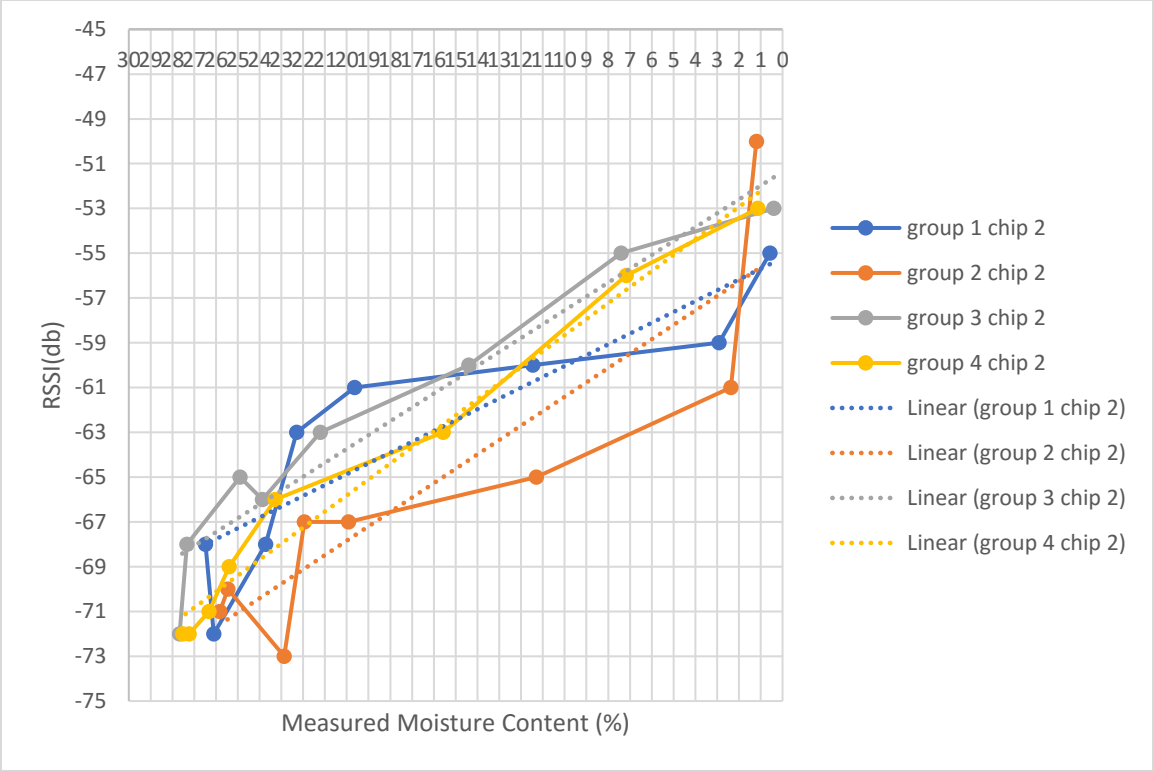

Figure 7.4.8: Graphical analysis of RSSI data of chip 2 from second-round test.

Firstly, all groups in the two rounds of tests show a linear relationship between RSSI and measured moisture content. However, there is a significant difference of slope between the 2 tags which were embedded for each sample. This may be due to mutual interference between the two tags, especially when the sample was saturated, and the tags' signals were weak. When the sample was almost dry, the signal was strong enough for both tags to signal almost the same.

Moreover, the linear relationships of the two rounds of the tests are also different which is possibly because of the different test locations (ambient condition). Due to the shutdown of school (COVID 19), the second test was conducted in a location where the room

temperature was higher and the final moisture content of samples in the second test are lower than the first test.

7.5 Conclusion

This test confirms that beyond recognizing patterns of moisture, the FLIR E60 thermal imager can be calibrated to discern moisture content readings based on recorded surface temperature values. The linear relationship of measured moisture content ratio and ΔT/average T may be consulted for determining moisture content readings in different ambient conditions; however, the recorded values are limited to the accuracy of the tool. The FLIR E60 has an accuracy of ±2°C or 2% at 25°C. For such small differences in ΔT, that margin of error may exceed the instrument's capability of recording similar surface temperature values.

As for the RFID technique, there is also a linear relationship in the result of tests. The accuracy of the signal strength the reader receives is very low and not stable which means the result is constantly changing. Besides, the most significant problem is the sensitivity of the tag near-fields to interference. This interference ideally is the result of moisture in the area surrounding the tag. However, it can also result from many other factors. These may make the RFID hard to quantitively measure the moisture content in adobe walls in-situ, but in lab, it is feasible according to the linear relationship between RSSI and moisture content.

7.6 Recommendations for further testing

The testing methodology developed for this investigation provides an optimistic outlook for architectural conservators to use infrared thermography and RFID techniques as a non-destructive tool to determine moisture content readings in adobe structures. However, further testing and alterations to the procedure are needed to improve the methodology.

The length of time required for the preparation of the samples decreased the available to test within project time constraints. During the testing week, the room conditions varied with weather and an out-of-service air conditioning system. Months with lower variability in temperature and relative humidity would be beneficial to collect more information within isothermal data sets. Testing in the winter may help to improve environment stability because the room relative humidity is low and temperature easier to control. The low room relative humidity accelerates evaporation flux in samples with high moisture content values, which the infrared camera will detect as a greater temperature difference between surface temperature and the temperature of the room. This test should be run for a period longer than one week to account for variability in ambient conditions and understand values between similar data sets.

RFID tests need to be repeated multiple times to improve the accuracy. If the latest types of tags which are able to measure both and temperature and humidity can be obtained, the data of IRT and RFID can be corelated and calibrated with each other.

Bibliography

Andrae G. The measurement of moisture in concrete. Materialprufung 1973; 15(3): 95–97.

Avdelidis NP, Moropoulou A. Applications of infrared thermography for the investigation of historic structures. J Cultural Heritage 2004;5(1):119–27.

Aytun, A. 1981. “Earthen buildings in seismic areas of Turkey”. In Proceedings of the International Workshop on Earthen Buildings in Seismic Areas, Vol. II, 345–371. Albuquerque, NM: University of New Mexico Press.

Balaras CA, Argiriou AA. Infrared thermography for building diagnostics. Energy Build 2002;34(2):171–83.

Binici, H., Aksogan, O. and Shah, T. 2005. Investigation of fibre reinforced mud brick as a building material. Construction and Building Materials, 19(4): 313–318.

Brown, W. P., Robbins, R. C. and Clifton, R. J. 1979. Adobe II: Factors affecting the durability of adobe structures. Studies in Conservation, 24(1): 23–29.

Construction Industries Division of the Regulation and Licensing, “2003 New Mexico Earthen Building Materials Code, Title 14, Chapter 7, Part 4”

Dill MJ. A review of testing for moisture in building elements. Construction Industry Research and Information Association, London, 2000.

Domenica Paoletti, et al, “Preventive Thermographic Diagnosis of Historical Buildings for Consolidation,” Journal of Cultural Heritage Vol, 14 (2013), pp. 116-121.

Eidmann G, Savelsberg R, Blu¨mler P, Blu¨mich B. The NMR mouse, a mobile universal surface explorer. Journal of Magnetic Resonance Series A 1996; 122: 104–109.

Evan Oskierko – Jeznacki, “An Alternative Technique for Low-Cost, Non-Destructive Moisture Monitoring in Adobe Walls using Embedded RFID Technology”, Unpublished

Fridh, L; Eliasson, L; Bergström, D, 2018, “Precision and accuracy in moisture content determination of wood fuel chips using a handheld electric capacitance moisture meter”, Silva Fennica. Volume 52, Issue 5, p. 1.

Glaser H. Graphical method for investigation of diffusional processes. Kaltetechnik 1959; 11(10): 345–349

Hall, M. and Djerbib, Y. 2004. Moisture ingress in rammed earth: Part 1–The effect of the soil particle–size distribution on the rate of capillary suction. Construction and Building Materials, 18(4): 269–280.

Hammond, A. A. 1973. Prolonging the life of earth buildings in the tropics. Building Research & Information, 1(3): 154–163.

Huw Lloyd, technical director, Dr Jagjit Singh, "Environmental monitoring: inspection, investigative monitoring techniques for historic buildings and case studies - brief paper" Environmental Building Solutions Ltd, UK

Illampas, R; Ioannou, I; Charmpis, D, 2013, "Overview of the Pathology, Repair and Strengthening of Adobe Structures", International Journal of Architectural Heritage. Volume 7, Issue 2, pp. 165-188.

Knowler AE. On the measurement of the electrical resistance of porous materials. Proc Phys Soc 1927; 40: 37–40.

Lewis G. Harriman III, "Practical Aspects of Locating and Measuring Moisture in Buildings"

Newman AJ. The independent core method - a new technique for the determination of moisture content. Building Science 1974; 9: 309–313.

Pearson, G. T. 1994. Conservation of clay and chalk buildings, Shaftesbury, , UK: Donhead Publishing.

Qu, J. J., Cheng, G. D., Zhang, K. C., Wang, J. C., Zu, R. P. and Fang, H. Y. 2007. An experimental study of the mechanisms of freeze/thaw and wind erosion of ancient adobe buildings in Northwest China. Bulletin of Engineering Geology and the Environment, 66(2): 153–169.

S. G. Reynolds, 1970, "The Gravimetric method of Soil Moisture Determination" Journal of Hydrology 11 (1970) P258-273

Salles, F., Douillard, J. M., Denoyel, R., Bildstein, O., Jullien, M., Beurroies, I. and Van Damme, H. 2009. Hydration sequence of swelling clays: Evolutions of specific

surface area and hydration energy. Journal of Colloid and Interface Science, 333(10): 510–522.

UK Climate Impacts Programme. Climate change scenarios for the United Kingdom: The UKCIP02 Briefing Report. Tyndall Centre for Climate Change Research, Norwich, 2002.

Walker, P. 2002. Australian earth building handbook: HB195–2002, Sydney, Australia: Standards Australia.

Warren, J. 1998. Conservation of earth structures, Oxford, UK: Butterworth–Heinemann.

Index